Journal of Medicinal Chemistry

Article

pubs.acs.org/jmc

Design and in Vitro Activities of *N*-Alkyl-*N*-[(8-*R*-2,2-dimethyl-2*H*-chromen-6-yl)methyl]heteroarylsulfonamides, Novel, Small-Molecule Hypoxia Inducible Factor-1 Pathway Inhibitors and Anticancer Agents

Jiyoung Mun,[†] Adnan Abdul Jabbar,[‡] Narra Sarojini Devi,[‡] Shaoman Yin,[‡] Yingzhe Wang,[▽] Chalet Tan,[▽] Deborah Culver,[⊥] James P. Snyder,[⊥,#] Erwin G. Van Meir,*[,‡,§,∥] and Mark M. Goodman*[,†,∥]

[†]Department of Radiology and Imaging Sciences, Emory University CSI, Wesley Woods Health Center, 1841 Clifton Road, NE, Atlanta, Georgia 30329, United States

[‡]Department of Neurosurgery, [§]Hematology and Medical Oncology, Emory University School of Medicine, [∥]Winship Cancer Institute, [⊥]Emory Institute for Drug Development, and [#]Department of Chemistry, Emory University, Atlanta, Georgia 30322, United States

[▽]Department of Pharmaceutical Sciences, College of Pharmacy, Mercer University, Atlanta, Georgia 30341, United States

Supporting Information

ABSTRACT: The hypoxia inducible factor (HIF) pathway is an attractive target for cancer, as it controls tumor adaptation to growth under hypoxia and mediates chemotherapy and radiation resistance. We previously discovered 3,4-dimethoxy-*N*-[(2,2-dimethyl-2*H*-chromen-6-yl)methyl]-*N*-phenylbenzenesulfonamide as a novel, small-molecule HIF-1 pathway inhibitor in a high-throughput cell-based assay, but its in vivo delivery is hampered by poor aqueous solubility (0.009 μM in water; log $P_{7.4}$ = 3.7). Here we describe the synthesis of 12 *N*-alkyl-*N*-[(8-*R*-2,2-dimethyl-2*H*-chromen-6-yl)methyl]heteroarylsulfonamides, which were designed to possess optimal lipophilicities and aqueous solubilities by in silico calculations. Experimental log $P_{7.4}$ values of 8 of the 12 new analogs ranged from 1.2−3.1. Aqueous solubilities of three analogs were measured, among which the most soluble *N*-[(8-methoxy-2,2-dimethyl-2*H*-chromen-6-yl)methyl]-*N*-(propan-2-yl)pyridine-2-sulfonamide had an aqueous solubility of 80 μM, e.g., a solubility improvement of ∼9000-fold. The pharmacological optimization had limited impact on drug efficacy as the compounds retained IC_{50} values at or below 5 μM in our HIF-dependent reporter assay.

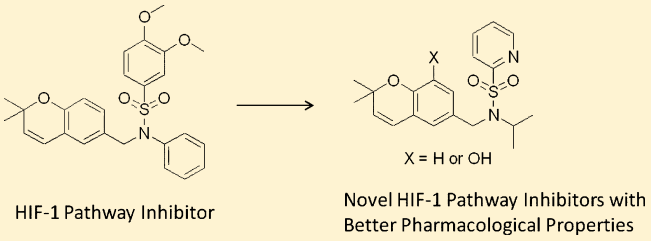

1. INTRODUCTION

The vasculature associated with fast proliferating solid tumors is abnormal, which limits efficient oxygen supply and renders the tumor tissue hypoxic.[1−3] The presence of hypoxic areas in solid cancers has been correlated with resistance to chemotherapy and radiation treatment. Intratumoral hypoxia induces hypoxia inducible factors (HIFs), transcription factors that activate genes controlling mechanisms such as glycolysis, erythropoiesis, angiogenesis, and cell motility, which can benefit the survival of cancer cells.[4−11] HIFs can also influence the self-renewal of cancer stem-like cells (CSCs)[12−14] and be activated in response to growth factors, oncogenes, and inactivation of tumor suppressor genes.[4−7]

HIFs are heterodimeric protein complexes, composed of HIF-α and HIF-β subunits, which then associate with cofactors such as p300 and CBP to form active transcription factors. The regulation of HIFs largely occurs at the protein level, and is dependent upon the synthesis and stability of the HIF-α subunits. Under normoxia, HIF-α subunits are hydroxylated at proline residues by oxygen-dependent prolyl hydroxylases (PHDs), which mediates recognition by the Von Hippel−Lindau (VHL) E3 ubiquitin ligase complex and rapid degradation by the proteasome. Under hypoxia, HIF-α subunits are stabilized due to the inhibition of proline hydroxylation, and a functional HIF transcriptional complex is assembled, translocates to the nucleus, and transcribes genes that contain DNA sequences called hypoxia response elements (HREs).[4−7] Elevated levels of HIF-1α have been correlated with poor prognosis of patients with glioblastoma (GBM), breast, pancreatic, colon, and metastatic lung cancers.[15−24]

Hypoxic tumor and HIF-1 have been evaluated as targets for anticancer therapy using a variety of approaches.[25−30] While the differential function of HIF-1 and HIF-2 isoforms is still under investigation,[7,31] both are associated with brain cancer stem-like cells,[13,14] and most studies suggest that one or both isoforms need targeting, depending on tumor and cancer type. Therefore, tumor cells overexpressing HIF represent an important target for

Received: January 3, 2012
Published: June 29, 2012

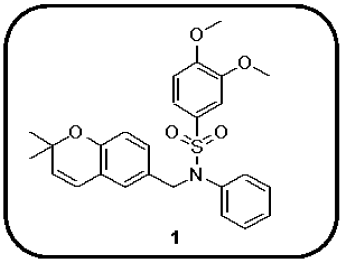

(A) 3,4-Dimethoxy-*N*-[(2,2-dimethyl-*2H*-chromen-6-yl)methyl]-*N*-phenylbenzenesulfonamide (**1**)

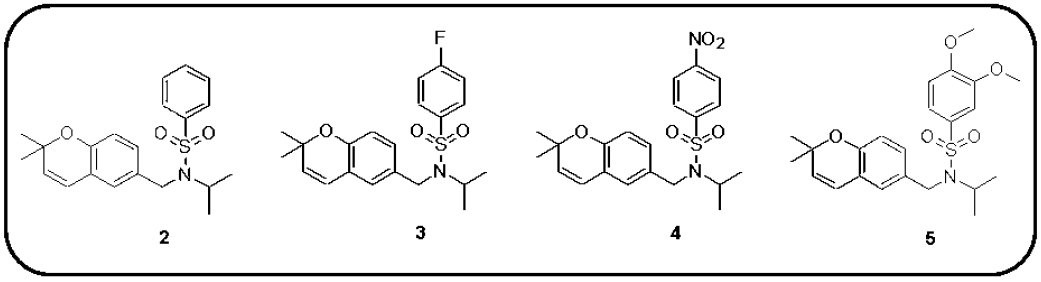

(B) *N*-[(2,2-dimethyl-*2H*-chromen-6-yl)methyl]-*N*-(propan-2-yl)arylsulfonamide (**2**, **3**, **4**, **5**)

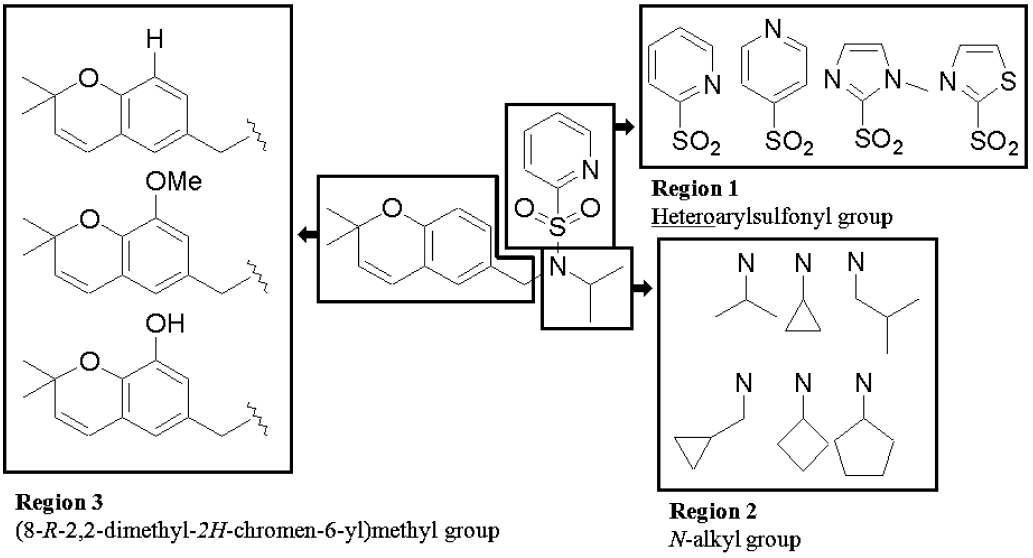

(C) *N*-alkyl-*N*-[(8-*R*-2,2-dimethyl-*2H*-chromen-6-yl)methyl]heteroarylsulfonamides

Figure 1. Design of *N*-alkyl-*N*-[(8-*R*-2,2-dimethyl-2*H*-chromen-6-yl)methyl]heteroarylsulfonamides.

antitumor therapy.[31−33] A number of existing chemotherapeutics can alter HIF activity as a result of their pleiotropic effects, including 2ME2, 17-DMAG, 17-AAG, camptothecin, PX-478, and YC-1.[34−40] Most of the agents studied affect HIF indirectly via the inhibition of microtubule polymerization, Hsp90, topoisomerase I, thioredoxin 1, or other unknown mechanisms.[41,42] A search for more specific inhibitors used a screen targeting the interaction of HIF with the key transcriptional coactivator p300. The small molecule chetomin was identified but later found to act as a general inhibitor of zinc ion binding proteins[43] and was abandoned due to unacceptable toxicity in mice.[44] A recent study suggests that acriflavine, an antitrypanocidal, antibacterial, and antiviral agent interferes with HIF-1α and -1β dimerization and possibly other signaling pathways such as NF-κB.[45] It is too early to determine which agent affecting the HIF pathway will have the best antitumor efficacy and safety profile. It is also desirable to develop several agents that can interfere with HIF transcription in different ways so that we are prepared for the development of tumor resistance against single targeted sites.

We recently discovered 3,4-dimethoxy-*N*-[(2,2-dimethyl-2*H*-chromene-6-yl)methyl]-*N*-phenylbenzenesulfonamide (**1**)[46] as a novel, small-molecule HIF-1 pathway inhibitor in a high-throughput screening among 10 000 molecular compounds that were based on a 2,2-dimethyl-2*H*-chromene structure as a naturally occurring biologically active lead moiety.[40,47−49]

Our ongoing investigations have identified the CH1 domain of p300/CBP as the putative target of **1**, and its binding is expected to disrupt the formation of the transcriptional complex among HIF-1α, HIF-1β, and p300/CBP under hypoxia.[50,51] **1** showed anticancer activity in vivo in brain, eye, and pancreatic cancer mouse models; however, it necessitated delivery in a formulation (Cremophor:ethanol = 1:1) due to poor aqueous solubility

dx.doi.org/10.1021/jm300752n | *J. Med. Chem.* 2012, 55, 6738−6750

Table 1. Molecular Weights (M_w) and log *P* and log S_w Values of 3,4-Dimethoxy-*N*-[(2,2-dimethyl-2*H*-chromene-6-yl)methyl]-*N*-phenylbenzenesulfonamide (1),[46] *N*-[(2,2-Dimethyl-2*H*-chromen-6-yl)methyl]-*N*-(propan-2-yl)arylsulfonamides (2, 3, 4, 5),[54] and Twelve *N*-Alkyl-*N*-[(8-*R*-2,2-dimethyl-2*H*-chromen-6-yl)methyl]heteroarylsulfonamides by in Silico Calculations[a]

Compound Name	Chemical Structure	M_w (Molecular Weight)	*log P* (Lipophilicity)	*log* S_w (Aqueous Solubility)
1	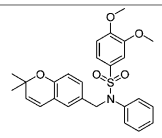	465.61	4.94	-6.05
2	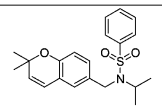	371.54	4.37	-4.78
3	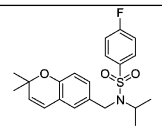	389.53	4.56	-4.79
4	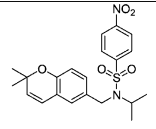	416.54	4.31	-5.07
5	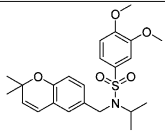	431.60	4.13	-4.81
6a	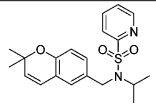	372.53	3.64	-3.73
6b	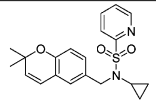	370.51	3.42	-3.89
6c	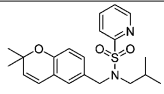	386.56	4.03	-3.91

Compound Name	Chemical Structure	M_w (Molecular Weight)	*log P* (Lipophilicity)	*log* S_w (Aqueous Solubility)
6d	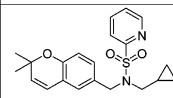	384.54	3.75	-4.11
6e	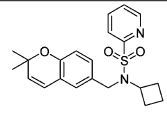	384.54	3.77	-3.94
6f	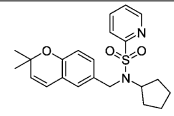	398.57	4.18	-4.20
6g	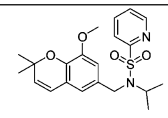	402.56	3.54	-3.74
6h	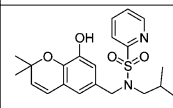	402.56	3.59	-3.45
6i	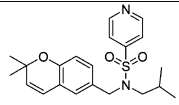	386.56	3.78	-3.95
6j	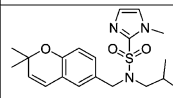	389.57	3.45	-3.16
6k	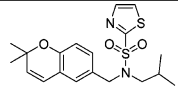	392.59	4.08	-4.19
6l	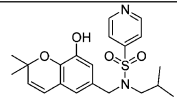	402.56	3.37	-3.39

[a]The values were calculated by online software, ALOGPS 2.1 (Virtual Computational Chemistry Laboratory, http://www.vcclab.org).[57−62]

(0.009 μM).[52,53] To develop analogs of **1** with improved aqueous solubility, we previously investigated structure−activity relationships of 15 lipophilic analogs and selected *N*-[(2,2-dimethyl-2*H*-chromene-6-yl)methyl]-*N*-(propan-2-yl)arylsulfonamides as the molecular motifs for further modifications described in the current study.[54]

Here we designed *N*-alkyl-*N*-[(8-*R*-2,2-dimethyl-2*H*-chromen-6-yl)methyl]heteroarylsulfonamides (abbreviated hereafter as "heteroarylsulfonamides") to possess molecular weights and estimated log *P* and log S_w values optimal for lead compounds in drug discovery.[55,56] Twelve heteroarylsulfonamides were synthesized, and their inhibition potency against the transcriptional activity of HIF-1, effect on HIF-1α synthesis and stability, physicochemical properties, metabolic stabilities, and cytotoxicities in human glioma and fibroblast cells were measured.

2. RESULTS

2.1. Design of *N*-Alkyl-*N*-[(8-*R*-2,2-dimethyl-2*H*-chromen-6-yl)methyl]heteroarylsulfonamides. The heteroarylsulfonamides were designed on the basis of *N*-[(2,2-dimethyl-2*H*-chromen-6-yl)methyl]-*N*-(propan-2-yl)arylsulfonamides (**2**−**5**, Figure 1). Heteroarylsulfonyl groups were used in region 1 instead of arylsulfonyl groups to increase aqueous solubility. Small alkyl groups were used in region 2, to retain biological activity without abruptly increasing lipophilicity. The 2,2-dimethyl-2*H*-chromene structure in region 3 was diversified at the C-8 position by adding a hydroxyl or methoxy group due to synthetic feasibility. A hydroxyl group is advantageous in that it can be an anchor for functional groups to further increase the diversity and structural flexibility of the compounds.

Twelve heteroarylsulfonamides (**6a**−**6l**) were selected for synthesis (Table 1) Their molecular weights range from 371 to 403 g/mol, log *P* values from 3.4 to 4.2, and log S_w values from −4.2 to −3.2, which are optimal for lead compounds in drug discovery.[55,56]

2.2. Synthesis of *N*-Alkyl-*N*-[(8-*R*-2,2-dimethyl-2*H*-chromen-6-yl)methyl] heteroarylsulfonamides. The chromene ring of 8-*R*-2,2-dimethyl-2*H*-chromene-6-carbaldehydes (**7a**, **7b**) was formed by Claisen cyclization of the propargyl ether, 3-*R*-4-[(2-methylbut-3-yn-2-yl)oxy]benzaldehyde, as described

dx.doi.org/10.1021/jm300752n | J. Med. Chem. 2012, 55, 6738−6750

previously.[54,63] The *N*-[(8-*R*-2,2-dimethyl-2*H*-chromen-6-yl)-methyl]alkylamines (**8a**−**8g**) were synthesized from **7a** and **7b** by acid-catalyzed imine formation and then subsequent reduction with diisobutylaluminum hydride (DIBAL).

The final *N*-alkyl-*N*-[(8-*R*-2,2-dimethyl-2*H*-chromen-6-yl)-methyl]heteroarylsulfonamides (**6a**−**6g**, **6i**−**6k**) were synthesized from **8a**−**8g** and heteroarylsulfonyl chlorides. Several synthetic methods have been developed for the preparation of heteroarylsulfonyl chlorides, which are unstable molecules. These include low-temperature oxidative chlorination of thioheterocycles with chlorine gas,[64] chlorination of heteroaromatic methyl sulfides with sulfuryl chloride,[65] oxidation of heteroaromatic thiols in a cosolvent of methylene chloride and 1 N aqueous hydrochloric acid containing 25 wt % calcium chloride with aqueous sodium hypochlorite,[66] and oxidation of heteroaromatic thiols in concentrated sulfuric acid with aqueous sodium hypochlorite.[67,68] We synthesized heteroarylsulfonyl chlorides by the last method due to facile reaction conditions. Slow addition of aqueous sodium hypochlorite solution to the reaction mixture was crucial for the high yield of the reaction, since low temperature has to be maintained during the highly exothermic reaction to prevent decomposition of the resulting heteroarylsulfonyl chlorides. The final heteroarylsulfonamides were formed in the presence of triethylamine at 40 °C (refluxing methylene chloride) in the case of pyridine-2-sulfonyl chloride, but in *N*,*N*-diisopropylethylamine (NIEA, Hünig's base) at 0 °C for pyridine-4-sulfonyl chloride, 1-methyl-1*H*-imidazol-2-sulfonyl chloride, and 1,3-thiazol-2-sulfonyl chloride, since the latter heteroarylsulfonyl chlorides decomposed above 0 °C. For the reactions at 0 °C, the reaction mixture was gradually concentrated by argon gas to accelerate the reactions (Scheme 1).

Insertion of a hydroxyl group at the C-8 position of the 2,2-dimethyl-2*H*-chromene ring was accomplished by chromenylation of 3,4-dihydroxybenzaldehyde with 3-methylbut-2-enal, for which the yield was low and not optimized.[69−71] The hydroxyl group at the C-8 position of the chromene ring was protected with methyl chloromethyl ether (MOMCl) to form a methoxymethyl ether, which was deprotected by 6 N aqueous HCl mixed with 1 equiv of tetrahydrofuran (THF) at the end of the synthesis (Scheme 2).

2.3. Inhibition of HIF Transcriptional Activity. The effects of the 12 heteroarylsulfonamides on HIF transcriptional activity under hypoxia were measured by determining the luciferase activity present in LN229-V6R cells, which contain a stably integrated hypoxia/HIF inducible luciferase reporter gene.[40,46,54] As a control for the absence of inhibition on luciferase enzyme per se, we also tested **1** and five heteroarylsulfonamides in LN229-Lux cells that contain a constitutive luciferase reporter gene driven by a retroviral LTR promoter. An Hsp90 inhibitor, 17-DMAG, and **1** were used as positive controls. 17-DMAG inhibited both reporter cell lines due to its known cytotoxicity; whereas **1** and heteroarylsulfonamides reduced luciferase activity only in LN229-V6R cells under hypoxia. The heteroarylsulfonamides decreased HIF-1 activity in a dose-dependent fashion with IC_{50} values below (**6a**, **6b**, **6d**−**6f**, **6h**, **6i**, **6l**) or close to 5 μM (**6c**, **6g**, **6j**, **6k**) (Figure 2).

Region 1 of **6c**, **6i**, **6j**, and **6k** was diversified with pyridine-2-sulfonyl, pyridine-4-sulfonyl, 1-methyl-1*H*-imidazole-2-sulfonyl, and thiazole-2-sulfonyl groups, among which the pyridine-4-sulfonyl group of **6i** showed the strongest HIF reporter inhibition. However, the pyridine-2-sulfonyl group of **6h** showed stronger inhibition than the pyridine-4-sulfonyl group of **6l**, when a hydroxyl group replaces the C-8 hydrogen in region 3.

Scheme 1. Synthesis of *N*-Alkyl-*N*-[(8-*R*-2,2-dimethyl-2*H*-chromen-6-yl)methyl]heteroarylsulfonamides[a]

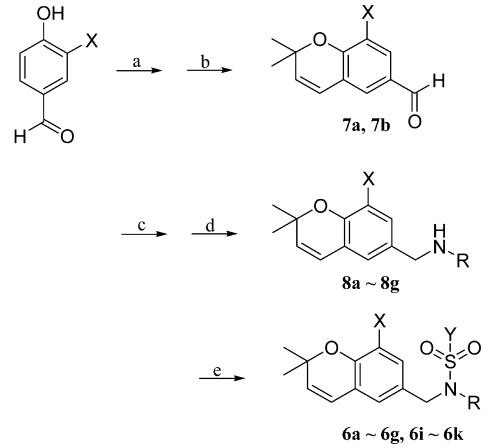

X = hydrogen, methoxy
Y = 2-pyridine, 4-pyridine, 2-thiazole, 1-methyl-1*H*-imidazole-2-
R = 1-methylethyl, cyclopropyl, 2-methylpropyl, cyclopropylmethyl, cyclobutyl, cyclopentyl

[a]Reagents and conditions: (a) 3-chloro-3-methyl-1-butyne, 4 N aq NaOH, DMF, 60 °C, overnight; (b) *N*-methylpyrrolidone (NMP), reflux, overnight (15% in two steps); (c) alkylamine (propan-2-amine, cyclopropanamine, 2-methylpropan-1-amine, 1-cyclopropylmethanamine, cyclobuthanamine, cyclopenthanamine), *p*-toluenesulfonic acid monohydrate, methylene chloride, reflux, overnight; (d) diisobutylaluminum hydride (DIBAL), toluene, overnight (39−89% in two steps); (e) heteroarylsulfonyl chloride, triethylamine, methylene chloride, reflux, overnight, or heteroarylsulfonyl chloride, *N*,*N*-diisopropylethylamine, methylene chloride, 0 °C to room temperature, overnight (17−77%).

Region 2 of **6a**−**6f** was varied with propan-2-yl, cyclopropyl, 2-methylpropan-1-yl, cyclopropylmethyl, cyclobutyl, and cyclopentyl groups, among which cyclopropylmethyl of **6d** showed the strongest HIF reporter inhibition.

Region 3 of **6a** and **6g** was altered at the C-8 position of the 2,2-dimethyl-2*H*-chromene ring with a hydrogen and a methoxy group, and **6a** (hydrogen) showed the strongest inhibition. Region 3 of **6c** and **6i** was different at the same position with a hydrogen and a hydroxyl group. In this case, **6i** (hydroxyl) showed stronger inhibition at low concentration; however, dose-dependent inhibition increased more sharply for **6c** (hydrogen). Region 3 of **6i** and **6l** was modified in the same way as **6c** and **6g** with a hydrogen and a hydroxyl group, of which **6l** (hydroxyl) showed slightly stronger inhibition at low concentration; however, dose-dependent inhibition increased more sharply for **6i** (hydrogen).

2.4. Effect on HIF-1α Stability under Hypoxia. HIF-1 is a heterodimer of HIF-1α and HIF-1β subunits, which then associates with p300 or CBP cofactors to form an active transcriptional complex. We previously demonstrated that in contrast to many prior HIF inhibitors, **1** does not antagonize hypoxia-induced HIF-1α expression under concentrations at which it blocks HIF transcription in the reporter assay.[46] To determine whether the heteroarylsulfonamides retain this property, we determined the levels of HIF-1α protein under hypoxia in LN229-V6R cells. For these experiments we selected **6a**, **6g**, and **6l** because the three compounds exhibited different degrees of HRE reporter inhibition and possess structural diversities at the C-8 position of the chromene ring. We investigated if the levels of HIF-1α protein would correlate with transcriptional inhibition of the HRE reporter by the

dx.doi.org/10.1021/jm300752n | *J. Med. Chem.* 2012, 55, 6738−6750

Scheme 2. Synthesis of *N*-[(8-Hydroxy-2,2-dimethyl-2*H*-chromen-6-yl)methyl]-*N*-(2-methylpropan-1-yl)pyridine-2-sulfonamide (6h) and *N*-[(8-Hydroxy-2,2-dimethyl-2*H*-chromen-6-yl)methyl]-*N*-(2-methylpropan-1-yl)pyridine-4-sulfonamide (6l)[a]

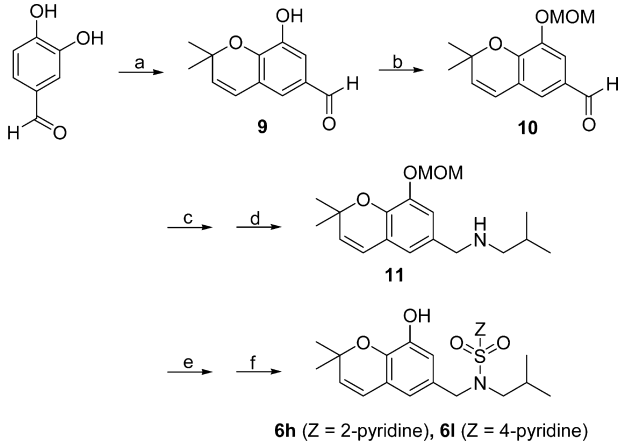

[a]Reagents and conditions: (a) 3-methylbut-2-enal, pyridinium trifluoromethanesulfonate, pyridine, reflux, 2 days (2.4%); (b) chloromethyl methyl ether, *N*,*N*-diisopropylethylamine, tetrahydrofuran, reflux, overnight (38%); (c) 2-methylpropan-1-amine, *p*-toluenesulfonic acid monohydrate, methylene chloride, reflux, overnight; (d) 1 M diisobutylaluminium hydride (DIBAL) in toluene, methylene chloride/toluene (1/2 (v/v)), overnight (13% in two steps); (e) pyridine-2-sulfonyl chloride, triethylamine, methylene chloride, reflux, overnight (for **6h**), or pyridine-4-sulfonyl chloride, *N*,*N*-diisopropylethylamine, methylene chloride, 0 °C to room temperature, overnight (for **6l**); (f) 6 N aqueous HCl, tetrahydrofuran, 3 h (48–49% in two steps).

compounds. LN229-V6R cells were treated with the compounds at concentrations of 3, 6, 12, 25, 50, and 100 μM under hypoxia for 24 h, and then HIF-1α protein levels in the cell extracts were examined by Western blotting. **6a** had no effect on HIF-1α levels at all concentrations tested, except for a slight reduction at the highest concentration (100 μM). **6g** and **6l** decreased HIF-1α levels in a dose-dependent fashion starting from 12 and 25 μM, respectively (Figure 3). In comparison, in the above HRE-mediated luciferase assays HIF-1 transcriptional activity was inhibited completely by **6a** and by more than 60–80% by **6g** and **6l** when tested at 10 μM (Figure 2). These results indicate that **6a**, **6g**, and **6l** most likely inhibit HIF transcription in a protein stability independent way similar to **1**. The reduction in HIF-1α levels afforded by all three compounds at 100 μM may reflect nonspecific cytotoxicity.

2.5. Physicochemical Properties and Metabolic Stability. Experimental determinations of log $P_{7.4}$, aqueous solubility, and metabolic stability of a selected number of the heteroarylsulfonamides were performed to further characterize the compounds (Table 2).

log $P_{7.4}$ was measured by either the shake flask method (**6a**, **6g**) or the HPLC method (**1**, **6b–6f**, **6h–6l**) according to OECD guidlines.[72] Most compounds followed the trends predicted by in silico calculations, and the measured values were smaller than the predicted values by 1.0–1.5. When a methoxy group or hydroxyl group is placed at the C-8 position of the chromene ring instead of a hydrogen, as in **6g**, **6h**, and **6l**, the log $P_{7.4}$ value decreased by more than 2 from the predicted values to result in 1.2–1.3. The presence of a 2-methylpropan-2-yl group in region 2 conferred high log $P_{7.4}$ values, and heteroarylsulfonyl groups in region 1 also affected log $P_{7.4}$ values, as shown for **6c**, **6i**, **6j**, and **6k**.

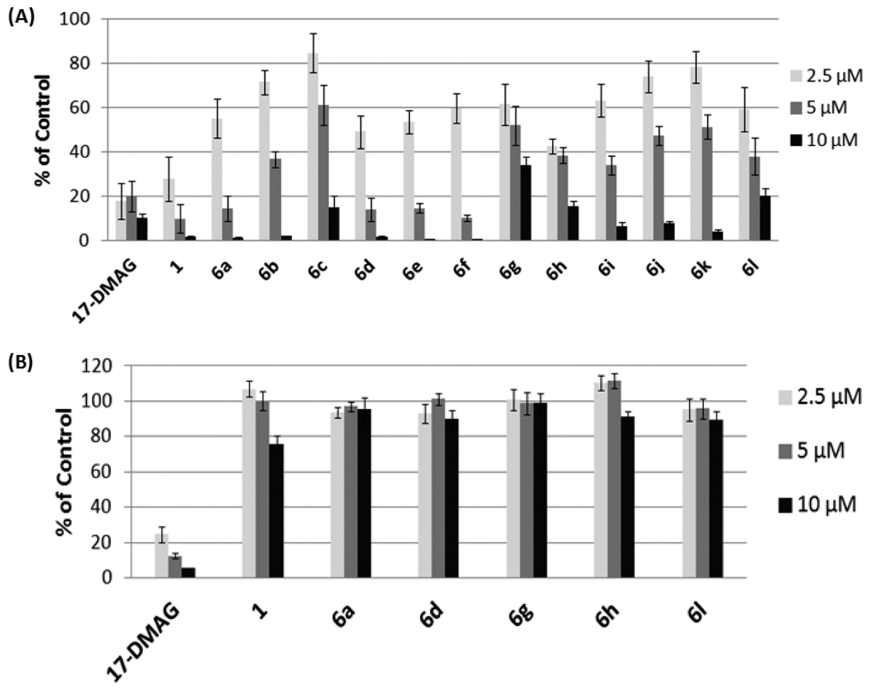

Figure 2. Reporter assays measuring luciferase activity in extracts from cells containing hypoxia-inducible (A) or constitutive (B) luciferase reporter genes following treatment with the indicated heteroarylsulfonamides. Results are plotted as percent of luciferase activity found in extracts of untreated cells used as controls. (A) Luciferase activity in extracts of LN229-V6R cells, which contain a HIF-inducible luciferase reporter gene. The cells were grown under hypoxia to activate HIF. (B) Luciferase activity in extracts of LN229-Lux cells, which contain a constitutively expressed luciferase reporter gene. Results shown are from cells grown under normoxia; similar results were obtained under hypoxia.

dx.doi.org/10.1021/jm300752n | *J. Med. Chem.* 2012, 55, 6738–6750

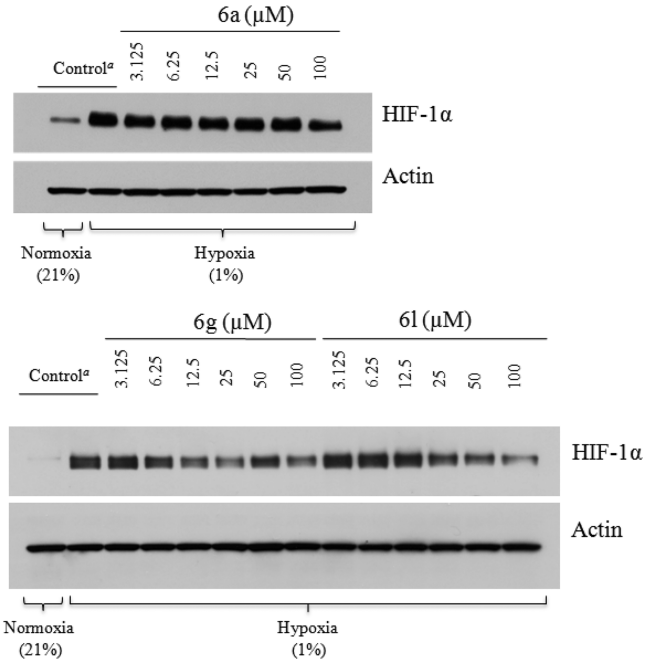

Figure 3. Measurement of HIF-1α levels in LN229-V6R cells in response to various doses of **6a**, **6g**, and **6l** by Western blot analysis. [a]Controls contain vehicle only (1% DMSO).

Table 2. log $P_{7.4}$, Aqueous Solubility, and Hepatic Metabolic Stability of *N*-Alkyl-*N*-[(8-*R*-2,2-dimethyl-2*H*-chromen-6-yl)-methyl]heteroarylsulfonamides

compd	log $P_{7.4}$	aqueous solubility (n = 3) (μg/mL, μM)	half-life[b] (h)	remaining HIF-1 activity at 2.5 μM: % of control	rank
1	3.7	0.003[a] ± 0.001, 0.009 ± 0.003	11	28	1
6a	2.0	0.3[a] ± 0.1, 1 ± 0.1	20	55	5
6b	3.0	nd[c]	nd	71	10
6c	4.1	nd	nd	85	13
6d	3.1	0.1[a] ± 0.02, 0.2 ± 0.07	13	49	3
6e	3.0	nd	nd	53	4
6f	3.8	nd	nd	60	7
6g	1.3	22 ± 16, 80 ± 36	15	61	8
6h	1.3	nd	15	43	2
6i	3.6	nd	nd	63	9
6j	3.1	nd	nd	74	11
6k	4.4	nd	nd	78	12
6l	1.2	nd	nd	59	6

[a]Aqueous solubility by laser nephelometry was measured as follows. **1**: pH 7.4, <15 μg/mL; pH 5.0, <15 μg/mL; pH 3.0, <15 μg/mL. **6a**: pH 7.4, <15 μg/mL; pH 5.0, 16 μg/mL; pH 3.0, 17 μg/mL. **6d**: pH 7.4, <15 μg. [b]Half-life was measured in homogenized mouse liver in PBS [1:2 (w/v)]. [c]The notation "nd" signifies that an experiment was not done.

Aqueous solubilities of **1**, **6a**, **6d**, and **6g** were quantified by HPLC coupled with a UV detector[67] on saturated aqueous suspensions after filtration with a polytetrafluoroethylene (PTFE) filter (pore size 0.2 μm). **6a** and **6d** were chosen due to their strong activity in the HRE-reporter assay, and **6g** was picked to evaluate the influence of the methoxy group attached to the C-8 position of the chromene ring. Aqueous solubilities of **6a**, **6d**, and **6g** are, respectively, 100, 20, and 9000 times better than that of **1**, which are consistent with the log S_w predictions for **6a** and **6d**. The substitution of hydrogen with a methoxy group at the C-8 position of the chromene ring increased the aqueous solubility by 90 times (compare **6a** and **6g**). Additional measurements of aqueous solubility of **1** and **6a** were performed by laser nephelometry at three different pHs (3.0, 5.0, and 7.4). pH did not affect aqueous solubility of **1**; however, low pH increased the aqueous solubility of **6a** by 50–60 times (pH 5.0, pH 3.0) due to the presence of the basic nitrogen in the pyridin-2-sulfonyl group in region 1.

Metabolic stabilities of **1**, **6a**, **6d**, **6g**, and **6l** were measured in mouse plasma and homogenates of mouse liver in PBS [1:2 (w/v)]. The concentrations of all compounds did not decrease by more than 1% when the compounds were incubated in mouse plasma at 37 °C for 24 h, which indicated the absence of degradation or metabolism in plasma. All compounds underwent ex vivo hepatic metabolism with the half-lives shown in Table 2, in which **1** showed the fastest and **6a** the slowest metabolism. (See a graph in the Supporting Information.)

2.6. Inhibition of Cell Viability/Proliferation. To determine whether **6a**, **6g**, and **6l** altered tumor cell growth in culture, we performed sulforhodamine B (SRB) assays in LN229-V6R glioma cells in 3 days, and to further examine the cell growth inhibitory activity of **6a**, **6g**, and **6l** in an independent biological assay, we performed clonogenicity assays in LN229 human glioblastoma cells and HFF-1 immortalized human fibroblasts, over a period of 14 days. IC_{50} values (μM) of SRB and clonogenicity assays are presented in Table 3.

2.6.1. Sulforhodamine B (SRB) Assay.[66] LN229-V6R cells (5×10^3 cells/well) were seeded and cultured under normoxia for 24 h, and cell densities were measured. The cells were then treated with serially diluted **6a**, **6g**, and **6l** (1.56–100 μM; 1% DMSO final in culture medium) under normoxia or hypoxia for 72 h. The three heteroarylsulfonamides showed stronger cytotoxicity under normoxia than under hypoxia. The IC_{50} values of cytotoxicity of the three heteroarylsulfonamides under hypoxia were over 100 μM in 3 days, whereas all of them decreased HRE-reporter activity by 60–95% at 10 μM in 1 day.

2.6.2. Clonogenicity Assays. **6a**, **6g**, and **6l** showed stronger inhibition of cell proliferation under normoxia than under hypoxia in both of glioblastoma and fibroblast cell lines, which was similar to results of SRB assays. The cytotoxicity profiles of each compound against glioblastoma (LN229) and fibroblast (HFF-1) cell lines were similar, suggesting nonspecific cytotoxicities. **6l** displayed the strongest cytotoxicity in both of the two cell lines.

3. DISCUSSION AND CONCLUSIONS

We previously discovered **1** as a potent HIF-1 pathway inhibitor with a cell-based high-throughput assay.[46] **1** contains a 2,2-dimethyl-2*H*-chromene ring found in many natural products. For example, 2,2-dimethyl-2*H*-chromene-based molecules isolated from *Blepharispermum subsessile* and the leaves of *Piper aduncum L.* have antifungal, antibacterial, and trypanocidal activities.[73−75] The chromenes extracted from the leaves of *Melicope lunu-ankenda* have antipyretic, analgesic, anti-inflammatory, and antioxidant activities.[76] Further structure–activity relationship (SAR) studies on **1** showed that *N*-[(2,2-dimethyl-2*H*-chromen-6-yl)methyl]-*N*-(propan-2-yl)arylsulfonamides possess strong HIF-1 pathway inhibition and are amenable for further chemical optimization.[54]

dx.doi.org/10.1021/jm300752n | J. Med. Chem. 2012, 55, 6738–6750

Table 3. IC_{50} (μM) Values of SRB and Clonogenecity Assays[a]

(A) SRB Assay		
compd	condition	IC_{50} (μM)
6a	normoxia	100
	hypoxia	126
6g	normoxia	73
	hypoxia	146
6l	normoxia	92
	hypoxia	113

(B) Clonogenecity Assays			
compd	cell line	condition	IC_{50} (μM)
6a	LN229	normoxia	82
		hypoxia	134
	HFF-1	normoxia	62
		hypoxia	93
6g	LN229	normoxia	69
		hypoxia	>100
	HFF-1	normoxia	55
		hypoxia	>100
6l	LN229	normoxia	23
		hypoxia	30
	HFF-1	normoxia	22
		hypoxia	40

[a]IC_{50} values were calculated by fitting the data to exponential or polinominal equations with $R^2 \geq 0.8$. The graphs are presented in the Supporting Information (S5).

Here, we improved the prior compounds by designing a series of 2,2-dimethyl-2*H*-chromene-based heteroarylsulfonamides with the purpose of decreasing lipophilicity and increasing aqueous solubility. We modified the *N*-[(2,2-dimethyl-2*H*-chromen-6-yl)methyl]-*N*-(propan-2-yl)-arylsulfonamides by substituting the arylsulfonyl group in region 1 with heteroarylsulfonyl groups such as pyridine-2-sulfonyl, pyridine-4-sulfonyl, 1-methyl-1*H*-imidazole-2-sulfonyl, and thiazole-2-sulfonyl groups; by replacing the propan-2-yl group in region 2 with short alkyl groups that mainly consist of small cyclic alkyl groups; and by derivatizing the chromene moiety at the C-8 position in region 3. Twelve heteroarylsulfonamides were designed to possess optimal log *P* and log S_w values by in silico calculations and subsequently synthesized. All 12 heteroarylsulfonamides show inhibition of HIF-1 transcription in a reporter assay at low micromolar concentrations, and the mechanism of action appeared independent of alteration in HIF-1α protein expression. Our ongoing studies suggest that the mechanism of action of **1** involves the disruption of the interaction between HIF-1α and its cofactors p300/CBP by antagonizing the CH1 domain of p300.[50,51] We expect that heteroarylsulfonamides will possess similar biological activities; however, this will need further experimental validation.

Eight heteroarylsulfonamides showed lower log $P_{7.4}$ values ranging from 1.2 to 3.1 versus 3.7 for **1**. Increased aqueous solubilities were achieved for compounds **6a**, **6d**, and **6g**, which were 100, 20, and 9000 times more soluble than **1**, respectively. The stabilities of **6a**, **6d**, **6g**, and **6l** in mouse plasma were similar to that of the parent compound **1**; however, they exhibited longer half-lives in homogenized mouse liver, ranging from 13 to 20 h, compared with 11 h for **1**, which suggests that they will likely be more resistant to in vivo hepatic metabolism than **1**.

We developed novel heteroarylsulfonamides to optimize pharmacological properties of **1**, and investigated their structure−activity relationships to improve HIF-1 inhibitory activity simultaneously. Six-membered heteroaryl groups in region 1, a propan-2-amine in region 2, and a (6-hydroxy-2,2-dimethyl-2*H*-chromen-6-yl)methyl group in region 3 were the best selections to increase the aqueous solubility and HIF-1 inhibition and decrease lipophilicity. 1-Cyclopropylmethanamine and cyclobutanamine in region 2 showed better HIF-1 inhibition than propan-2-amine; however, lipophilicity, aqueous solubility, and metabolic stability made the latter group the superior choice. A functional group at the C-8 of the chromene ring significantly affected physicochemical properties and HIF-1 inhibition, so a further investigation of derivatization is required.

In conclusion, the novel heteroarylsulfonamides we synthesized have dramatically improved aqueous solubility, less lipophilicity, and slightly better stability, while retaining much of the bioactivity of the parent compound.

The next step toward the clinical translation of the heteroarylsulfonamides will be to optimize their pharmacological properties in vivo and test their antitumor properties in animal models for cancer.

4. EXPERIMENTAL SECTION

4.1. Synthesis. Reagents were purchased from Sigma-Aldrich, Alfa Aesor, and Fisher Scientific. Anhydrous solvents were purchased from Sigma-Aldrich. Glassware was oven-dried at 200 °C and cooled under argon to room temperature. All reactions were performed under argon gas. Column chromatography was performed with silica gel 60 (particle size 40−63 μm) with less than 4 psi of argon pressure.

Thin-layer chromatography was performed with TLC silica gel 60 F_{254}, and organic compounds were visualized by UV light (254 nm), iodine vapor, phosphomolybdic acid [10% (w/v) in ethanol] staining with heating, and ninhydrin solution with heating for amines. NMR spectroscopy was recorded by Varian INOVA 400, Mercury 300, and VNMRS 400 spectrometers. Mass spectroscopy was obtained by a JEOL JMS-SX102/SX102A/E instrument. HPLC was accomplished with a Waters 1525 binary HPLC pump coupled with a Waters 2487 Dual λ absorbance detector, and data were processed by Waters Breeze GPC Software. Dual wavelengths of 254 and 280 nm were used for UV absorbance measurements. The running time of HPLC for each compound was 20 min, and the peaks were integrated after 3.5 min.

The purity of **6a**−**6l** was over 95%, which was determined by the percent area of its UV absorbance peak at 254 nm by two different HPLC systems. In the first HPLC system, a symmetry C_{18} column (WAT045905, 5 μm, 4.6 × 150 mm) was used with the eluent 70:30:0.1 = methanol:water:triethylamine at a flow rate of 2 mL/min. In the second HPLC system, a Nova-Pak C_{18} column (WAT011695, 4 μm, 3.9 × 300 mm) was used with the eluent 60:40:0.1 = (90% ethanol, 5% methanol, 5% 2-propanol):water:triethylamine at a flow rate at 0.8 mL/min. An alcohol mix of 90% ethanol, 5% methanol, and 5% 2-propanol was used instead of pure ethanol due to an institutional regulation limiting ethanol purchase.

*2,2-Dimethyl-2H-chromene-6-carbaldehyde or 8-Methoxy-2,2-dimethyl-2H-chromene-6-carbaldehyde (**7a**, **7b**).* An aqueous sodium hydroxide solution (4 N, 5 mL) was added to a solution of 4-hydroxybenzaldehyde (2.38 g, 19.5 mmol) and 3-chloro-3-methyl-1-butyne (1 g, 9.75 mmol) in 8 mL of dimethylformamide (DMF), to form a binary solution. The reaction mixture was stirred vigorously at 60 °C overnight. After cooling, 20 mL of water was added to the reaction mixture, which was extracted with diethyl ether (30 mL × 3). The combined organic phase was washed with 40 mL of 1 N aqueous sodium hydroxide and then brine, dried with anhydrous magnesium sulfate, and concentrated in vacuo. Formation of crude 4-[(2-methylbut-3-yn-2-yl)oxy]benzaldehyde was confirmed by TLC with ethyl acetate/hexane (1/8) and NMR. ^{1}H NMR ($CDCl_3$): δ 1.73

dx.doi.org/10.1021/jm300752n | J. Med. Chem. 2012, 55, 6738−6750

(s, 6H), 2.67 (s, 1H), 7.34 (d, J = 8.8 Hz, 1H), 7.83 (d, J = 8.8 Hz, 1H), 9.91 (s, 1H).

Crude 4-[(2-methylbut-3-yn-2-yl)oxy]benzaldehyde was dissolved in 10 mL of *N*-methylpyrrolidone (NMP, bp = 202−204 °C) and refluxed overnight. After cooling to room temperature, 80 mL of water was added to the solution, which was extracted with diethyl ether (100 mL × 3). The combined organic phase was washed with brine, dried with anhydrous magnesium sulfate, and concentrated in vacuo. **7a** was purified by silica gel chromatography with ethyl acetate/hexane (1/8) as a viscous yellowish liquid (565 mg, 15% yield). ^{1}H NMR ($CDCl_3$): δ 1.46 (s, 6H), 5.68 (d, J = 9.9 Hz, 1H), 6.36 (d, J = 9.9 Hz, 1H), 6.85 (d, J = 8.05 Hz, 1H), 7.50 (d, J = 2.37 Hz, 1H), 7.63 (dd, J = 8.52, 1.89 Hz, 1H), 9.83 (s, 1H). HRMS (m/z): M^+ calcd 189.09101, found 189.09071.

7b was synthesized by the same method as **7a**. Vanillin (3 g, 20 mmol) and 3-chloro-3-methyl-1-butyne (1 g, 10 mmol) were used as starting materials. **7b** was purified by silica gel chromatography with ethyl acetate/hexane (1/6) as a white solid (204 mg, 5% in two steps)

3-Methoxy-4-[(2-methylbut-3-yn-2-yl)oxy]benzaldehyde. ^{1}H NMR ($CDCl_3$): δ 1.75 (s, 6H), 2.63 (s, 1H), 3.90 (s, 3H), 7.43−7.40 (m, 2H), 7.64 (d, J = 8.79 Hz, 1H).

*8-Methoxy-2,2-dimethyl-2H-chromene-6-carbaldehyde (**7b**).* ^{1}H NMR ($CDCl_3$): δ 1.51 (s, 6H), 3.93 (s, 3H), 5.70 (d, J = 9.78 Hz, 1H), 6.37 (d, J = 9.78 Hz, 1H), 7.17 (d, J = 1.96 Hz, 1H), 7.32 (d, J = 1.96 Hz, 1H), 9.81 (s, 1H). HRMS (m/z): M^+ calcd 219.10157, found 219.10124.

*N-[(2,2-Dimethyl-2H-chromen-6-yl)methyl]propan-2-amine (**8a**).* **7a** (102 mg, 0.54 mmol) was dissolved in 2 mL of anhydrous methylene chloride, to which *p*-toluenesulfonic acid monohydrate (20 mg, 0.1 mmol) and propan-2-amine (1 mL, 12 mmol) were added. The reaction mixture was refluxed overnight and then concentrated in vacuo. The NMR of the crude product confirmed a complete conversion of the aldehyde, **7a**, to the corresponding imine by disappearance of the aldehyde proton peak, 9.83 ppm (s, 1H), and appearance of the imine proton peak, 8.19 ppm (s, 1H).

The crude imine was suspended in 3 mL of toluene, to which 1 M diisobutylaluminum hydride in toluene (DIBAL, 2.5 mL, 2.5 mmol) was added slowly to control vigorous bubbling. The reaction mixture was stirred overnight at room temperature, and then 20 mL of 1 N aqueous hydrochloric acid was added to the reaction mixture slowly, to quench the reduction. The resulting emulsion was basified with concentrated aqueous sodium carbonate solution. The reaction mixture was extracted with ethyl acetate (20 mL × 3). The combined organic phase was washed with brine, dried with anhydrous magnesium sulfate, and then concentrated in vacuo. **8a** was purified by silica gel chromatography with triethylamine/methanol/methylene chloride (1/1/100) as a viscous oil (111 mg, 89% in two steps). ^{1}H NMR ($CDCl_3$): δ 1.1 (d, J = 6.15 Hz, 6H), 1.4 (s, 6H), 2.85 (septet, J = 6.45 Hz, 1H), 3.66 (s, 2H), 5.6 (d, J = 9.96 Hz, 1H), 6.3 (d, J = 9.67 Hz, 1H), 6.72 (d, J = 8.2 Hz, 1H), 6.95 (d, J = 2.05 Hz, 1H), 7.04 (dd, J = 2.34, 7.91 Hz, 1H).

Other amines (**8b**−**8g**) were synthesized by the same method as **8a**. The imine formation was confirmed by disappearance of the aldehyde proton peak [9.83 ppm (**7a**) or 9.81 ppm (**7b**)] and appearance of the corresponding imine peak [8.1−8.3 ppm (s, 1H)]. The amines were synthesized by reduction of the corresponding imines.

*N-[(2,2-Dimethyl-2H-chromen-6-yl)methyl]cyclopropanamine (**8b**).* Yield = 37% in two steps. ^{1}H NMR ($CDCl_3$): δ 0.93 (t, J = 7.33 Hz, 2H), 1.43 (s, 6H), 1.56 (sextet, J = 7.33 Hz, 1H), 2.61 (t, J = 7.33 Hz, 2H), 3.70 (s, 2H), 5.61 (d, J = 9.67 Hz, 1H), 6.31 (d, J = 9.67 Hz, 1H), 6.73 (d, J = 8.20 Hz, 1H), 6.97 (d, J = 2.05 Hz, 1H), 7.06 (dd, J = 2.05, 8.20 Hz, 1H).

*N-[(2,2-Dimethyl-2H-chromen-6-yl)methyl]-2-methylpropan-1-amine (**8c**).* Yield = 30% in two steps. ^{1}H NMR ($CDCl_3$): δ 0.92 (d, J = 6.45 Hz, 6H), 1.43 (s, 6H), 1.79 (septet, J = 6.45, 6.74 Hz, 1H), 2.44 (d, J = 7.03 Hz, 2H), 3.68 (s, 2H), 5.61 (d, J = 9.96 Hz, 1H), 6.32 (d, J = 9.96 Hz, 1H), 6.73 (d, J = 8.20 Hz, 1H), 6.96 (d, J = 2.05 Hz, 1H), 7.05 (dd, J = 2.05, 7.91 Hz, 1H).

*1-Cyclopropyl-N-[(2,2-dimethyl-2H-chromen-6-yl)methyl]-methamine (**8d**).* Yield = 77% in two steps. ^{1}H NMR ($CDCl_3$): δ 0.13 (m, 2H), 0.47−0.53 (m, 2H), 0.97−1.05 (m, 1H), 1.42 (s, 6H), 2.51 (d, J = 6.74 Hz, 2H), 3.73 (s, 2H), 5.61 (d, J = 9.67 Hz, 1H), 6.32 (d, J = 9.67 Hz, 1H), 6.73 (d, J = 8.20 Hz, 1H), 6.98 (d, J = 2.05 Hz, 1H), 7.07 (dd, J = 2.05, 8.20 Hz, 1H).

*N-[(2,2-Dimethyl-2H-chromen-6-yl)methyl]cyclobutanamine (**8e**).* Yield = 60% in two steps. ^{1}H NMR ($CDCl_3$): δ 1.42 (s, 6H), 1.59−1.75 (m, 5H), 2.19−2.27 (m, 2H), 3.25−3.35 (m, 1H), 3.60 (s, 2H), 5.60 (d, J = 9.67 Hz, 1H), 6.31 (d, J = 9.67 Hz, 1H), 6.72 (d, J = 8.20 Hz, 1H), 6.95 (d, J = 2.05 Hz, 1H), 7.04 (dd, J = 2.05, 8.20 Hz, 1H).

*N-[(2,2-Dimethyl-2H-chromen-6-yl)methyl]cyclopentanamine (**8f**).* Yield = 67% in two steps. ^{1}H NMR ($CDCl_3$): δ 1.36−1.42 (m, 3H), 1.42 (s, 6H), 1.51−1.56 (m, 2H), 1.68−1.73 (m, 2H), 1.84−1.89 (m, 2H), 3.12 (quintet, J = 6.74 Hz, 1H), 3.67 (s, 2H), 5.60 (d, J = 9.67 Hz, 1H), 6.31 (d, J = 9.96 Hz, 1H), 6.72 (d, J = 8.20 Hz, 1H), 6.96 (d, J = 2.05 Hz, 1H), 7.05 (dd, J = 2.05, 8.20 Hz, 1H).

*N-[8-Methoxy-(2,2-dimethyl-2H-chromen-6-yl)methyl]propan-2-amine (**8g**).* Yield = 39% in two steps. ^{1}H NMR ($CDCl_3$): δ 1.11 (d, J = 6.15 Hz, 6H), 1.46 (s, 6H), 2.88 (septet, J = 6.15 Hz, 1H), 3.68 (s, 2H), 3.86 (s, 3H), 5.61 (d, J = 9.67 Hz, 1H), 6.28 (d, J = 9.96 Hz, 1H), 6.60 (s, 1H), 6.78 (s, 1H).

*N-[(2,2-Dimethyl-2H-chromen-6-yl)methyl]-N-(propan-2-yl)-pyridine-2-sulfonamide (**6a**). Pyridine-2-sulfonyl Chloride.* 2-Mercaptopyridine (126 mg, 1 mmol) was dissolved in 5 mL of concentrated sulfuric acid to form a yellow solution, which was cooled to around −15 °C with a sodium chloride/ice (1/3) bath. Aqueous sodium hypochlorite solution (10−15%, 11 mL, 15−20 mmol) was added to the solution slowly enough to maintain the internal temperature of the reaction mixture below 10 °C, with vigorous stirring. The reaction mixture was stirred at 0 °C for 1 hour and then 10 mL of water was added, which was then extracted with methylene chloride (20 mL × 3). The combined organic phase was washed with water, dried with anhydrous magnesium sulfate, and then concentrated in vacuo. Pyridine-2-sulfonyl chloride (145 mg, 72%) was produced as a yellowish viscous liquid. ^{1}H NMR ($CDCl_3$): δ 7.684−7.729 (m, 1H), 8.043−8.143 (m, 2H), 8.84 (d, J = 4.10 Hz, 1H).

Freshly prepared pyridine-2-sulfonyl chloride (100 mg, 0.6 mmol) was added to a solution of **8a** (25 mg, 0.1 mmol) and triethylamine (0.5 mL, 3.6 mmol) in 0.8 mL of methylene chloride. The reaction mixture was refluxed overnight and then concentrated in vacuo. **6a** (31 mg, 77%) was purified by silica gel chromatography with ethyl acetate/hexane (1/1). ^{1}H NMR ($CDCl_3$): δ 1.03 (d, J = 6.74 Hz, 6H), 1.42 (s, 6H), 4.27 (septet, J = 6.74 Hz, 1H), 4.45 (s, 2H), 5.61 (d, J = 9.67 Hz, 1H), 6.30 (d, J = 9.67 Hz, 1H), 6.68 (d, J = 8.21 Hz, 1H), 7.04 (d, J = 2.05 Hz, 1H), 7.10 (dd, J = 2.05, 8.20 Hz, 1H), 7.38−7.47 (m, 1H), 7.81−7.96 (m, 2H), 8.7 (d, J = 4.40 Hz, 1H). HRMS (m/z): $[M + Na]^+$ calcd 395.13999, found 395.14017. HPLC-1: t_R = 4.5 min, purity = 98%. HPLC-2: t_R = 6.5 min, purity = 99%.

Other heteroarylsulfonamides containing a pyridine-2-sulfonyl group were synthesized by the same method as that of **6a**.

*N-Cyclopropyl-N-[(2,2-dimethyl-2H-chromen-6-yl)methyl]-pyridine-2-sulfonamide (**6b**).* Purification was by silica gel chromatography with ethyl acetate/hexane (2/3). Yield = 24%. ^{1}H NMR ($CDCl_3$): δ 0.725 (t, J = 7.33 Hz, 2H), 1.35−1.43 (m, 1H), 3.23 (dd, J = small as broadening of peaks, 7.62 Hz, 2H), 4.44 (s, 2H), 5.61 (d, J = 9.96 Hz, 1H), 6.27 (d, J = 9.97 Hz,1H), 6.68 (d, J = 8.20 Hz, 1H), 6.93 (d, J = 1.76 Hz, 1H), 7.01 (dd, J = 2.05, 8.20 Hz, 1H), 7.47 (ddd, J = 0.88,4.69, 7.32 Hz, 1H), 7.85−7.99 (m, 2H), 8.70 (d, J = 4.69 Hz, 1H). HRMS (m/z): $[M + Na]^+$ calcd 393.12488, found 395.14008. HPLC-1: t_R = 5.1 min, purity = 100%. HPLC-2: t_R = 6.8 min, purity = 97%.

*N-[(2,2-Dimethyl-2H-chromen-6-yl)methyl]-N-(2-methylpropyl)-pyridine-2-sulfonamide (**6c**).* Purification was by silica gel chromatography with ethyl acetate/hexane (1/4). Yield = 60%. ^{1}H NMR ($CDCl_3$): δ 0.76 (d, J = 6.74 Hz, 6H), 1.42 (s, 6H), 1.74 (septet, J = 7.03 Hz, 1H), 3.11 (d, J = 7.325 Hz, 2H), 4.42 (s, 2H), 5.60 (d, J = 9.67 Hz, 1H), 6.24 (d, J = 9.67 Hz, 1H), 6.65 (d, J = 8.20 Hz, 1H), 6.87 (d, J = 2.05 Hz, 1H), 6.96 (dd, J = 2.05, 8.20 Hz, 1H), 7.45 (ddd, J = 1.17, 4.69, 7.62 Hz, 1H), 7.865 (td, J = 1.76, 7.62 Hz,1H), 7.95 (d, J = 7.62 Hz, 1H), 8.69 (d, J = 4.69 Hz, 1H). HRMS (m/z): $[M + Na]^+$ calcd 409.15564, found 409.15649. HPLC-1: t_R = 6.8 min, purity = 100%. HPLC-2: t_R = 8.4 min, purity = 97%.

dx.doi.org/10.1021/jm300752n | *J. Med. Chem.* 2012, 55, 6738−6750

*N-(Cyclopropylmethyl)-N-[(2,2-dimethyl-2H-chromen-6-yl)-methyl]pyridine-2-sulfonamide (**6d**).* Purification was by silica gel chromatography with ethyl acetate/hexane (1/2). Yield = 24%. ^{1}H NMR ($CDCl_3$): δ 0.0115 (d, J = 5.27 Hz, 2H), 0.301 (d, J = 7.62 Hz, 2H), 0.67−0.825 (m, 1H), 1.425 (s, 6H), 3.17 (d, J = 6.74 Hz, 2H), 4.58 (s, 2H), 5.61 (d, J = 9.67 Hz, 1H), 6.28 (d, J = 9.67 Hz, 1H), 6.69 (d, J = 8.21 Hz, 1H), 6.975 (s, 1H), 7.04 (d, J = 7.91 Hz, 1H), 7.47 (dd, J = 4.98, 7.62 Hz, 1H), 7.88 (t, J = 7.62 Hz, 1H), 7.99 (d, J = 7.62 Hz, 1H), 8.71 (d, J = 4.69 Hz, 1H). HRMS (m/z): $[M + Na]^+$ calcd 407.13999, found 407.14046. HPLC-1: t_R = 5.7 min, purity = 100%. HPLC-2: t_R = 7.5 min, purity = 95%.

*N-(Cyclobutyl)-N-[(2,2-dimethyl-2H-chromen-6-yl)methyl]-pyridine-2-sulfonamide (**6e**).* Purification was by silica gel chromatography with ethyl acetate/hexane (1/2). Yield = 65%. ^{1}H NMR ($CDCl_3$): δ 1.42 (s, 6H), 1.42−2.04 (m, 6H), 4.31−4.39 (m, 1H), 4.51 (s, 2H), 5.61 (d, J = 9.96 Hz, 1H), 6.30 (d, J = 9.67 Hz, 1H), 6.69 (d, J = 8.20 Hz, 1H), 7.00 (s, 1H), 7.06 (dd, J = 2.05, 8.205 Hz, 1H), 7.43−7.48 (m, 1H), 7.82−7.94 (m, 2H), 8.69 (d, J = 3.81 Hz, 1H). HRMS (m/z): $[M + Na]^+$ calcd 407.13999, found 407.14034. HPLC-1: t_R = 5.6 min, purity = 100%. HPLC-2: t_R = 7.1 min, purity = 96%.

*N-(Cyclopentyl)-N-[(2,2-dimethyl-2H-chromen-6-yl)methyl]-pyridine-2-sulfonamide (**6f**).* Purification was by silica gel chromatography with ethyl acetate/hexane (1/4). Yield = 16%. ^{1}H NMR ($CDCl_3$): δ 1.26−1.59 (m, 8H), 1.43 (s, 6H), 4.31−4.40 (m, 1H), 4.48 (s, 2H), 5.61 (d, J = 9.67 Hz, 1H), 6.30 (d, J = 9.67 Hz, 1H), 6.69 (d, J = 8.21 Hz, 1H), 7.03 (s, 1H), 7.07 (d, J = 8.50 Hz, 1H), 7.44−7.48 (m, 1H), 7.83−7.94 (m, 2H), 8.71 (d, J = 4.69 Hz, 1H). HRMS (m/z): $[M + Na]^+$ calcd 421.15564, found 421.15577. HPLC-1: t_R = 7.3 min, purity = 100%. HPLC-2: t_R = 8.4 min, purity = 96%.

*N-[(8-Methoxy-2,2-dimethyl-2H-chromen-6-yl)methyl]pyridine-2-sulfonamide (**6g**).* Purification was by silica gel chromatography with ethyl acetate/hexane (2/1). Yield = 23%. ^{1}H NMR ($CDCl_3$): δ 1.05 (d, J = 6.74 Hz, 6H), 1.47 (s, 6H), 3.84 (s, 3H), 4.27 (septet, J = 6.74 Hz, 1H), 4.45 (s, 2H), 5.61 (d, J = 9.96 Hz, 1H), 6.27 (d, J = 9.96 Hz, 1H), 6.62 (s, 1H), 6.88 (s, 1H), 7.43−7.48 (m, 1H), 7.82−7.93 (m, 2H), 8.70 (d, J = 4.40 Hz, 1H). HRMS (m/z): $[M + Na]^+$ calcd 425.15055, found 425.15089. HPLC-1: flow rate 2 mL/min, t_R = 2.9 min, purity = 97%; flow rate 1 mL/min, t_R = 5.6 min, purity = 99%. HPLC-2: t_R = 5.1 min, purity = 100%.

*N-[(2,2-Dimethyl-2H-chromen-6-yl)methyl]-N-(2-methylpropyl)-pyridine-4-sulfonamide (**6i**). Pyridine-4-sulfonyl Chloride.* Pyridine-4-sulfonyl, 1,3-thiazole-2-sulfonyl, and 1-methyl-1*H*-imidazole-2-sulfonyl chloride were synthesized by the same method as that of pyridine-2-sulfonyl chloride. They were used immediately after synthesis due to their instabilities at temperatures above 0 °C. Ten theoretical equivalents of the sulfonyl chloride were synthesized, which were extracted with 10 mL of cold methylene chloride, washed with cold brine, and then dried with anhydrous magnesium sulfate. The sulfonyl chloride solution in methylene chloride was immersed in ice−water bath and concentrated with argon flow until the volume was reduced to 3 mL.

8a (25 mg, 0.1 mmol) was dissolved in 0.8 mL of methylene chloride, to which 0.5 mL of *N*,*N*-diisopropylethylamine (DIEA, 0.5 mL, 3 mmol) was added and cooled to 0 °C. Ten equivalents of freshly prepared pyridine-4-sulfonyl chloride was added to the reaction mixture slowly, which was stirred at 0 °C for 3 h with slow argon flow. **6i** (25 mg, 63%) was purified by silica gel chromatography with ethyl acetate/hexane (1/5). ^{1}H NMR ($CDCl_3$): δ 0.78 (d, J = 6.74 Hz, 6H), 1.43 (s, 6H), 1.72−1.82 (m, 1H), 2.96 (d, J = 7.62 Hz, 2H), 4.27 (s, 2H), 5.62 (d, J = 9.96 Hz, 1H), 6.21 (d, J = 9.96 Hz, 1H), 6.68 (d, J = 7.91 Hz, 1H), 6.77 (d, J = 2.05 Hz, 1H), 6.91 (dd, J = 2.05, 8.50 Hz, 1H), 7.63 (d, J = 5.86 Hz, 1H), 8.82 (d, J = 6.15 Hz, 1H). HRMS (m/z): $[M + Na]^+$ calcd 386.16641, found 387.17447. HPLC-1: t_R = 6.5 min, purity = 98%. HPLC-2: t_R = 8.4 min, purity = 96%.

6j and **6k** were synthesized by the same method as **6i**.

*N-[(2,2-Dimethyl-2H-chromen-6-yl)methyl]-N-(2-methylpropyl)-1-methyl-1H-imidazole-2-sulfonamide (**6j**).* Purification was by silica gel chromatography with ethyl acetate/hexane (1/2). Yield = 58%. ^{1}H NMR ($CDCl_3$): δ 0.77 (d, J = 6.45 Hz, 6H), 1.43 (s, 6H), 1.63−1.70 (m, 1H), 3.20 (d, J = 7.62 Hz, 1H), 3.90 (s, 3H), 4.47 (s, 2H), 5.62 (d, J = 9.96 Hz, 1H), 6.29 (d, J = 9.67 Hz, 1H), 6.71 (d, J = 8.20 Hz, 1H), 6.93−6.94 (m, 2H), 7.04 (dd, J = 2.34, 8.20 Hz, 1H), 7.08 (d, J = 0.88 Hz, 1H). HRMS (m/z): $[M + Na]^+$ calcd 412.16654, found 412.16699. HPLC-1: t_R = 5.8 min, purity = 100%. HPLC-2: t_R = 8.7 min, purity = 97%.

*N-[(2,2-Dimethyl-2H-chromen-6-yl)methyl]-N-(2-methylpropyl)-1,3-thiazole-2-sulfonamide (**6k**).* Purification was by silica gel chromatography with ethyl acetate/hexane (1/2). Yield = 17%. ^{1}H NMR ($CDCl_3$): δ 0.79 (d, J = 6.45 Hz, 6H), 1.42 (s, 6H), 1.77−1.81 (m, 1H), 3.12 (d, J = 7.62 Hz, 2H), 4.43 (s, 2H), 5.62 (d, J = 9.96 Hz, 1H), 6.26 (d, J = 9.67 Hz, 1H), 6.68 (d, J = 8.20 Hz, 1H), 6.87 (d, J = 2.34 Hz, 1H), 6.97 (dd, J = 2.34, 8.20 Hz, 1H), 7.58 (d, J = 3.22 Hz, 1H), 7.95 (d, J = 3.22 Hz, 1H). HRMS (m/z): $[M + Na]^+$ calcd 415.11206, found 415.11253. HPLC-1: t_R = 8.0 min, purity = 100%. HPLC-2: t_R = 10 min, purity = 89%.

*8-Hydroxy-2,2-dimethyl-2H-chromene-6-carbaldehyde (**9**).* 3,4-Dihydroxybenzaldehyde (2.3 g, 17 mmol) and 3-methylbut-2-enal (1 mL, 10 mmol) were dissolved in 3 mL of pyridine and refluxed overnight. Pyridine was evaporated under vacuum, and the crude reaction mixture was dissolved in methylene chloride. **9** (103 mg, 2.4%) was purified with silica gel chromatography with ethyl acetate/hexane (1/50). ^{1}H NMR ($CDCl_3$): δ 1.50 (s, 6H), 5.70 (d, J = 10.1 Hz, 1H), 6.38 (d, J = 10.1 Hz, 1H), 7.15 (d, J = 2.14 Hz, 1H), 7.32 (d, J = 1.83 Hz, 1H), 9.78 (s, 1H).

*8-(Methoxymethoxy)-2,2-dimethyl-2H-chromene-6-carbaldehyde (**10**).* Chloromethyl methyl ether (4 mL, 5 mmol) was added to a solution of **9** (103 mg, 0.5 mmol) and *N*,*N*-diisopropylethylamine (0.2 mL, 1 mmol) in 4 mL of methylene chloride. The reaction mixture was refluxed overnight and concentrated in vacuo. **10** (48 mg, 38%) was purified with ethyl acetate/hexane (1/50). ^{1}H NMR ($CDCl_3$): δ 1.52 (s, 6H), 3.54 (s, 3H), 5.25 (s, 2H), 5.71 (d, J = 9.67 Hz, 1H), 6.38 (d, J = 9.96 Hz, 1H), 7.26 (d, J = 1.76 Hz, 1H), 7.52 (d, J = 1.76 Hz, 1H), 9.80 (s, 1H).

*N-[(8-Methoxymethoxy-2,2-dimethyl-2H-chromen-6-yl)methyl]-2-methylpropan-1-amine (**11**).* 2-Methylpropan-1-amine (0.5 mL, 5 mmol) and *p*-toluenesulfonic acid monohydrate (110 mg, 0.6 mmol) were added to a solution of **10** (143 mg, 0.6 mmol) in 5 mL of methylene chloride. The reaction mixture was refluxed overnight and concentrated in vacuo. Disappearance of the aldehyde peak at 9.80 ppm (s, 1H) and appearance of the imine peak at 8.07 ppm (s, 1H) were confirmed by NMR.

The crude product was dissolved in 3 mL of a mixture of methylene chloride and toluene [1/2 (v/v)], to which 1 M DIBAL in toluene (3 mL, 3 mmol) was added slowly to generate gentle bubbling. The reaction mixture was stirred for 5 h and 20 mL of 1 N aqueous HCl was added. The aqueous phase was extracted by methylene chloride (40 mL × 3). The combined organic layer was washed by brine, dried with magnesium sulfate, and then concentrated in vacuo.

11 (22 mg, 13%) was purified by silica gel chromatography with triethylamine/methanol/methylene chloride (1/3/100). ^{1}H NMR ($CDCl_3$): δ 0.91 (d, J = 3.13 Hz, 6H), 1.46 (s, 6H), 1.75−1.82 (m, 1H), 2.43 (d, J = 7.04 Hz, 2H), 3.53 (s, 3H), 3.66 (s, 2H), 5.20 (s, 2H), 5.62 (d, J = 9.78 Hz, 1H), 6.30 (d, J = 9.78 Hz, 1H), 6.69 (d, J = 1.96 Hz, 1H), 6.96 (d, J = 1.96 Hz, 1H).

*N-[(8-Hydroxy-2,2-dimethyl-2H-chromen-6-yl)methyl]-N-(propan-2-yl)pyridine-2-sulfonamide (**6h**).* **11** (30 mg, 0.1 mmol), pyridine-2-sulfonyl chloride (57 mg, 0.3 mmol), and *N*,*N*-diisopropylethylamine (0.2 mL, 1 mmol) were dissolved in 1 mL of methylene chloride and stirred at room temperature overnight. A completion of the reaction was confirmed by disappearance of the amine spot by TLC with triethylamine/methanol/methylene chloride (1/3/100) and appearance of the product spot by TLC with ethyl acetate/hexane (1/1). *N*-[(8-Methoxymethoxy-2,2-dimethyl-2*H*-chromen-6-yl)-methyl]-*N*-(propan-2-yl)pyridine-2-sulfonamide (31 mg, 70%) was purified by silica gel chromatography with ethyl acetate/hexane (1/1). ^{1}H NMR ($CDCl_3$): δ 0.78 (d, J = 6.45 Hz, 6H), 1.45 (s, 6H), 1.72−1.76 (m, 1H), 3.11 (d, J = 7.62 Hz, 2H), 3.50 (s, 3H), 4.40 (s, 2H), 5.14 (s, 2H), 5.62 (d, J = 9.96 Hz, 1H), 6.23 (d, J = 9.67 Hz, 1H), 6.60 (d, J = 1.76 Hz, 1H), 6.87 (d, J = 1.76 Hz, 1H), 7.43−7.47 (m, 1H), 7.84−7.96 (m, 2H), 8.68−8.7 (m, 1H).

dx.doi.org/10.1021/jm300752n | *J. Med. Chem.* 2012, 55, 6738−6750

N-[(8-Methoxymethoxy-2,2-dimethyl-2*H*-chromen-6-yl)methyl]-*N*-(propan-2-yl)pyridine-2-sulfonamide (31 mg, 0.07 mmol) was dissolved in a cosolvent of tetrahydrofuran (1 mL) and 6 N aqueous HCl (1 mL), and the reaction stirred for 3 h. Ten milliliters of water was added to the reaction mixture, and then tetrahydrofuran was evaporated. The remaining aqueous phase was extracted by methylene chloride (10 mL × 3), washed with brine, dried with anhydrous magnesium sulfate, and concentrated in vacuo. **6h** (19 mg, 49%) was purified by silica gel chromatography with ethyl acetate/hexane (1/1). ^{1}H NMR ($CDCl_3$): δ 0.77 (d, J = 6.45 Hz, 6H), 1.44 (s, 6H), 1.72−1.79 (m, 1H), 3.11 (d, J = 7.62 Hz, 2H), 4.39 (s, 2H), 5.61 (d, J = 9.67 Hz, 1H), 6.25 (d, J = 9.96 Hz, 1H), 6.50 (d, J = 1.76 Hz, 1H), 6.65 (d, J = 1.76 Hz, 1H), 7.43−7.47 (m, 1H), 7.84−7.97 (m, 2H), 8.69 (d, J = 4.40 Hz, 1H). HRMS (m/z): $[M + Na]^+$ calcd 425.15055, found 425.15091. HPLC-1: flow rate 2 mL/min, t_R = 2.9 min, purity = 100%; flow rate 1 mL/min, t_R = 5.6 min, purity = 100%. HPLC-2: t_R = 5.172 min, purity = 100%.

*N-[(8-Hydroxy-2,2-dimethyl-2H-chromen-6-yl)methyl]-N-(propan-2-yl)pyridine-4-sulfonamide (**6l**).* **6l** was synthesized by the same method as **6h**. Yield in two steps = 48%. ^{1}H NMR ($CDCl_3$): δ 0.80 (d, J = 6.74 Hz, 6H), 1.45 (s, 6H), 1.75−1.82 (m, 1H), 2.98 (d, J = 7.62 Hz, 2H), 4.24 (s, 2H), 5.62 (d, J = 9.67 Hz, 1H), 6.22 (d, J = 9.67 Hz, 1H), 6.39 (s, 1H), 6.60 (s, 1H), 7.62 (d, J = 5.86 Hz, 1H), 8.81 (d, J = 4.98 Hz, 1H). HRMS (m/z): $[M + Na]^+$ calcd 402.16133, found 403.16924. HPLC-1: flow rate 2 mL/min, t_R = 2.7 min, purity = 98%; flow rate 1 mL/min, t_R = 5.3 min, purity = 98%. HPLC-2: t_R = 5.532 min, purity = 100%.

4.2. Physicochemical Property Measurements. HPLC was measured with a Waters 1525 binary HPLC pump coupled with a Waters 2487 Dual λ absorbance detector, and the data were processed by Waters Breeze GPC Software; 254 and 280 nm were used for UV absorbance measurements. A Symmetry C_{18} (WAT045905, 5 μm, 4.6 × 150 mm) column was used with the eluent (70:30:0.1 = methanol:water:triethylamine) and a flow rate of 2 mL/min. Standard curves of **1**, **6a**, **6d**, and **6g** were constructed by injection of 20, 40, 60, 80, and 100 μL of standard solutions in 100% of methanol (0.01 mg/mL, 100% of methylene chloride for **1**) into the HPLC system. 1-Octanol (99%) was purchased from Alfa Aesar and phosphate buffer (0.2 M, pH 7.4) was purchased from Electron Microscopy Sciences.

4.2.1. log $P_{7.4}$ Measurements.[66] log $P_{7.4}$ values of **6a** and **6g** were measured according to the "OECD Guideline for Testing of Chemicals 107 adopted by the Council on July 27, 1995" (Method 1), and they were used as two reference materials for the rest of the compounds for which log $P_{7.4}$ values were measured by "OECD Guideline for Testing of Chemicals 117 adopted by the Council on April 13, 2004" (Method 2). The first method was more direct but too complicated to be applied for all compounds, so it was used only for **6a** and **6g**, which were then used as reference materials with aniline, benzene, toluene, and chlorobenzene in method 2 to increase its reliability.

Method 1. 1-Octanol (70 mL) was stirred vigorously with 30 mL of phosphate buffer at room temperature for 24 h, and the aqueous layer was discarded. The 1-octanol layer was washed with 30 mL of phosphate buffer. The same procedure was applied to 70 mL of phosphate buffer and 30 mL of 1-octanol. One to two milligrams of **6a** (or **6g**) was dissolved in 2 mL of 1-octanol saturated with phosphate buffer in 20 mL glass tubes in duplicate. Two milliliters of phosphate buffer saturated with 1-octanol was added to each tube, which were then tightly sealed with a cover. The mixtures were mechanically shaken for 15 min. The two layers were separated by centrifugation at 1500*g* for 10 min, 1 mL of each layer was transferred to a glass vial, and 0.1 mL of the 1-octanol layer was mixed with 5 mL of water and 10 mL of HPLC eluent (70:30:0.1 = methanol:water:triethylamine) to eliminate the 1-octanol effect on the retention time of HPLC, of which 0.5 mL was injected into the HPLC system. One-half milliliter of the aqueous layer was injected into the HPLC system. Peak areas at 254 nm were quantified by standard curves described above and used for the log $P_{7.4}$ calculations.

Method 2. All 13 compounds (**1**, **6a**−**6l**), aniline, benzene, toluene, and chlorobenzene were injected into the HPLC system described above. Retention times for solvent and each compound were obtained. Aniline, benzene, toluene, chlorobenzene, **6a**, and **6g** were used as reference compounds to obtain coefficients of a linear regression. log $P_{7.4}$ values of all other compounds were obtained by the linear regression equation constructed from the reference compounds.

4.2.2. Aqueous Solubility Measurements. **1** (1−2 mg) was placed in a 10 mL glass tube, to which 2 mL of distilled water was added. The suspension was sonicated for 30 min at room temperature and then centrifuged at 1500*g* at 20 °C for 5 min. The liquid was transferred to a clean glass tube and then filtered through a polytetrafluoroethylene (PTFE) filter (pore size 0.2 μm) slowly. Then 500 μL or 1 mL of the filtered clear solution was injected into the HPLC system, and peak areas at 254 nm were quntified using the standard curves described above. Three independent experiments were performed, and the average value was calculated. The same procedure was used for **6a**, **6d**, and **6g**.[77]

The aqueous solubilities of **1**, **6a**, and **6d**, were also independently measured by laser nephelometry. The compounds and an internal control were dissolved in 100% of DMSO to obtain a final concentration of 30 mg/mL to make stock solutions. A stock solution was serially diluted (concentration profile 30, 20, 15, 10, 7.5, 5, 2.5, 1.25, 0.63, 0.31, and 0.15 mg/mL) in test tubes with 100% of DMSO. The concentration profile was transferred to 96-well microplates (Costar black clear bottom) and serially diluted to a final concentration of 1% of DMSO and a final drug concentration of 300, 200, 150, 100, 75, 50, 25, 12, 6, 3, and 1.5 μg/mL with phosphate-buffered saline (pH 7.4, 5.0, or 3.0). The microplates were incubated for 90 min at ambient temperature. Laser nephelometry (NEPHELOstar, BMG Lab Technologies) was used to determine the point at which the solute began to precipitate out of solution.

4.3. Metabolism. **1**, **6a**, **6d**, **6g**, and **6h** (20 μM) were individually incubated with fresh mouse plasma or liver homogenate in phosphate-buffered saline (pH 7.4) [1/2 (w/v)] at 37 °C with constant shaking. At predetermined time points, 50 μL of plasma or liver homogenate sample was collected and extracted with 100 μL of acetonitrile. The supernatant was reduced to dryness under vacuum overnight and reconstituted in the HPLC mobile phase. The concentrations of each compound were individually determined using reverse phase HPLC methodology. The HPLC system (Waters, Milford, MA) consisted of a Waters 2795 pump, a Phenomenex (Torrance, CA) C_8 column (5 μm, 4.6 × 150 mm), and a Waters 996 photodiode array detector. As an internal standard, α-naphthoflavone was used at a concentration of 2 μM. The detection wavelengths for these compounds were as follows: **1** at 250 nm, both **6a** and **6d** at 264 nm, both **6g** and **6h** at 268 nm, and α-naphthoflavone at 281 nm. The linear range for the standard curves of all compounds was between 1 and 50 μM. All studies were done in triplicates.

4.4. HIF-Dependent Luciferase Reporter Assays. The LN229-V6R and LN229-Lux cells were maintained in Dulbecco's modified Eagle's medium (DMEM) (Mediatech, Herdon, VA) with 10% serum and antibiotics as previsouly described.[46] The cells (3×10^4 in 300 μL of DMEM medium) were seeded in each well of 48-well plates, and cultured under normoxia (21% O_2, 5% CO_2, and 74% N_2) for 24 h. Subsequently, the medium of each well was replaced with 300 μL of DMEM medium with 1% of DMSO, without (control) or with heteroarylsulfonamides, **6a**, **6g**, and **6l** (at 2.5, 5.0, and 10.0 μM); the plates were further incubated at 37 °C for 1 h and then transferred to a Steri-cycle CO_2 incubator (Thermo Forma, Model 370) under hypoxia (1% O_2, 5% CO_2, and 74% N_2) at 37 °C for another 24 h. The cells were washed with PBS buffer, and a cell extract was prepared after lysing them with 40 μL/well of lysis buffer (Promega, part# E1944) for 10 min. Protein suspensions (20 μL) from each well were mixed with 25 μL of luciferase assay substrate (Promega, Part# E151A), and luminescence was measured using a 20/20n luminometer (Turner BioSystems Inc.).[46] Assays were performed in triplicates.

4.5. Detection of Cellular HIF-1α Protein Levels by Western Blot Analyses. Western blots were prepared as previously described.[46] Briefly, LN229-V6R cells (2×10^5 in 2 mL of DMEM) were seeded in 35 mm cell culture dishes and cultured under normoxia for 24 h, and then new DMEM medium was added with 1% of DMSO and heteroarylsulfonamides **6a**, **6g**, and **6l** (at 3, 6, 12, 25, 50, or 100 μM). Dishes were incubated under normoxia at 37 °C for 1 h and then transferred to hypoxia (1% O_2) for 24 h.

Cells were lysed with 1× loading buffer [62.5 mM Tris-HCl (pH 6.8 at 25 °C), 2% (w/v) SDS, 50 μM 2-mercaptoethanol, 10% glycerol, 0.01% bromophenol blue], and proteins were separated by electrophoresis in a 4−12.5% Tris-HCl gradient gel (Bio-Rad, Richmond, CA). The proteins were transferred onto a nitrocellulose membrane and immunoblotted using anti-HIF-1α antibody (1:500 dilution BD biosciences, San Diego, CA) and anti-β-actin antibody (1:3000 dilution, Santa Cruz Biotechnologies, Santa Cruz, CA). The secondary horseradish peroxide-conjugated antibodies were added and horseradish peroxide activities were measured by enhanced chemiluminescence (Pierce, Rockford, IL).

Western blotting of each heteroarylsulfonamide (**6a**, **6g**, or **6l**) was repeated at least two times.

4.6. Measurement of Cell Growth by Sulforhodamine B (SRB) Colorimetric Assays.[78,79] LN229-V6R cells (2×10^3 in 200 μL of DMEM) were plated in each well of 48-well plates. Cells were allowed to attach under normoxia for 24 h, and then the medium was replaced with DMEM with 1% of DMSO containing **6a**, **6g**, or **6l** at a concentration of 3, 6, 12, 25, 50, or 100 μM. The plates were incubated under normoxia at 37 °C for 1 h and then under normoxia or hypoxia for 3 days. The individual assays were performed in quadruplicates or sextuplicates, and the experiments were repeated two independent times.

Cells were fixed by gentle addition of 50 μL of cold (4 °C) 10% of trichloroacetic acid (TCA) and then incubated at 4 °C for 1 h. Each well was washed with deionized water three times and then air-dried. Cells were stained for 30 min by addition of 100 μL of SRB solution [0.04% of SRB (w/v) in 1% of acetic acid (v/v)] to each well. Each well was washed five times with 1% of acetic acid and air-dried for 30 min. Bound dye was solubilized with 10 mM of Tris base (pH 10) prior to measuring the optical density at 564 nm in a BioTek Synergy HT.

4.7. Clonogenicity Assays. Heteroarylsulfonamides (**6a**, **6g**, **6l**) were dissolved in DMSO at 10 mM concentration and serially diluted in DMEM medium to reach final concentrations of 6.25, 12.5, 25, 50, and 100 μM with 1% of DMSO. Human glioma cells (LN229) or immortalized human fibroblasts (HFF-1) were seeded at 200 or 1000 cells per well in six-well plates and left to adhere on the plates under normoxia for 16 h. The media were removed, and DMEM media without (control) or with the compounds was added to each well. The plates were incubated under normoxia for 1 h and then under normoxia (21% O_2) or hypoxia (1% O_2) for 14 days. Thereafter, the cells were fixed, and the number of colonies in each was well revealed by staining with crystal violet (0.9%).

■ ASSOCIATED CONTENT

Ⓢ Supporting Information

NMR, HPLC, TLC, metabolic stability curve, and cytotoxicity curves of 12 *N*-alkyl-*N*-[(8-*R*-2,2-dimethyl-2*H*-chromen-6-yl)-methyl]heteroarylsulfonamides. This material is available free of charge via the Internet at http://pubs.acs.org.

■ AUTHOR INFORMATION

Corresponding Author

*M.G.: phone, (404) 727-9366; fax, (404) 712-5689; e-mail, mgoodma@emory.edu. E.G.V.M.: phone, (404) 778-5563; fax, (404) 778-5550; e-mail, evanmei@emory.edu.

Notes

The authors declare no competing financial interest.

■ ACKNOWLEDGMENTS

This research was supported by the National Institute of Health grants P50 CA128301-01A1, Emory Molecular and Translational Imaging Research Center (EMTIC)/In vivo Cellular and Molecular Imaging Centers (ICMIC) (to M.M.), P50 CA128301-01A1 Pilot Project #2 (to J.M.), R01 CA116804 (to E.G.V.M.), and V Foundation, Max Cure, and Samuel Waxman Cancer Research foundation grants (to E.G.V.M.). The authors greatly appreciate Dr. Ronald Voll and Dr. Stefan Kaluz for helpful discussions.

■ ABBREVIATIONS USED

HIF-1, hypoxia inducible factor-1; HRE, hypoxia response element; LN229-V6R, LN229 cells transfected with a vector, pBI-GL HRE V6R that contains a HRE-driven promoter and a luciferase reporter gene; DMSO, dimethyl sulfoxide; NMP, *N*-methyl-2-pyrrolidone

■ REFERENCES

(1) Brat, D. J.; Castellano-Sanchez, A. A.; Hunter, S. B.; Pecot, M.; Cohen, C.; Hammond, E. H.; Devi, S. N.; Kaur, B.; Van Meir, E. G. Pseudopalisades in glioblastoma are hypoxic, express extracellular matrix proteases, and are formed by an actively migrating cell population. *Cancer Res.* **2004**, *64*, 920−927.

(2) Kaur, B; Brat, D. J.; Devi, S. N.; Van Meir, E. G. Vasculostatin, a natural proteolytic fragment of brain angiogenesis inhibitor 1 is an anti-angiogenic and anti-tumorigenic factor. *Oncogene* **2005**, *24*, 3638−3642.

(3) Brat, D. J.; Castellano-Sanchez, A.; Kaur, B.; Van Meir, E. G. Genetic and biologic progression in astrocytomas and their relation to angiogenic dysregulation. *Adv. Anat. Pathol.* **2002**, *9*, 24−36.

(4) Giaccia, A.; Siim, B. G.; Johnson, R. S. HIF-1 as a target for drug development. *Nat. Rev. Drug Discovery* **2003**, *2*, 1−9.

(5) Melillo, G. Inhibiting hypoxia-inducible factor 1 for cancer therapy. *Mol. Cancer Res.* **2006**, *4*, 601−605.

(6) Semenza, G. L. Targeting HIF-1 for cancer therapy. *Nat. Rev. Cancer* **2003**, *3*, 721−732.

(7) Poon, E.; Harris, A. L.; Ashcroft, M. Targeting the hypoxia-inducible factor (HIF) pathway in cancer. *Expert Rev. Mol. Med.* **2009**, *11*, e26.

(8) Carmeliet, P.; Dor, Y.; Herbert, J.; Fukumura, D.; Brusselmans, K.; Dewerchin, M.; Neeman, M.; Bono, F.; Abramovitch, R.; Maxwell, P.; Koch, C. J.; Ratcliffe, P.; Moons, L.; Jain, R. K.; Collen, D.; Keshert, E. Role of HIF-1α in hypoxia-mediated apoptosis, cell proliferation and tumor angiogenesis. *Nature* **1998**, *395*, 485−490.

(9) Favaro, E.; Nardo, G.; Persano, L.; Masiero, M.; Moserle, L.; Zamarchi, R.; Rossi, E.; Esposito, G.; Plabani, M.; Sattler, U.; Mann, T.; Mueller-Klieser, W.; Ciminale, V.; Amadori, A.; Indraccolo, S. Hypoxia inducible factor-1α inactivation unveils a link between tumor cell metabolism and hypoxia-induced cell death. *Am. J. Pathol.* **2008**, *173*, 1186−1201.

(10) Kilic, M.; Kasperczyk, H.; Fulda, S.; Debatin, K. M. Role of hypoxia inducible factor-1 alpha in modulation of apoptosis resistance. *Oncogene* **2007**, *26*, 2027−2038.

(11) Schelter, F.; Gerg, M.; Halbgewachs, B.; Schaten, S.; Gorlach, A.; Schrotzlmair, F.; Kruger, A. Identification of a survival-independent metastasis-enhancing role of hypoxia-inducible factor-1α with a hypoxia-tolerant tumor cell line. *J. Biol. Chem.* **2010**, *285*, 26182−26189.

(12) Mendez, O.; Zavadil, J.; Esencay, M.; Lukyanov, Y.; Santovasi, D.; Wang, S.; Newcomb, E. W.; Zagzag, D. Knock down of HIF-1α in glioma cells reduces migration in vitro and invasion in vivo and impairs their ability to form tumor spheres. *Mol. Cancer* **2010**, *9*, 133−142.

(13) Hadjipanayis, C. G.; Van Meir, E. G. Tumor initiating cells in malignant gliomas: Biology and implications for therapy. *J. Mol. Med.* **2009**, *87*, 363−374.

(14) Hadjipanayis, C. G.; Van Meir, E. G. Brain tumor propagating cells: Biology, genetics, and targeted therapies. *Trends Mol. Med.* **2009**, *15*, 519−30.

(15) Kaur, B.; Khwaja, F. W.; Severson, E. A.; Matheny, S. L.; Brat, D. J.; Van Meir, E. G. Hypoxia and the hypoxia-inducible-factor pathway in glioma growth and angiogenesis. *Neuro-Oncology* **2005**, *7*, 106−121.

(16) Blum, R.; Jacob-Hirsch, J.; Amariglio, N.; Rechavi, G.; Kloog, Y. Ras inhibition in glioblastoma down-regulates hypoxia-inducible factor-1α, causing glycolysis shutdown and cell death. *Cancer Res.* **2005**, *65*, 999−1006.

(17) Hung, J. J.; Yang, M. H.; Hsu, H. S.; Hsu, W. H.; Liu, J. S.; Wu, K. J. Prognostic significance of hypoxia-inducible factor-1α, TWIST1 and Snail expression in resectable non-small cell lung cancer. *Thorax* **2009**, *64*, 1082−1089.
(18) Eul, B.; Rose, F.; Krick, S.; Savai, R.; Gyal, P.; Klepetko, W.; Grimminger, F.; Weissmann, N.; Seeger, W.; Hanze, J. Impact of HIF-1α and HIF-2α on proliferation and migration of human pulmonary artery fibroblasts in hypoxia. *FASEB J.* **2006**, *20*, 163−165.
(19) Rohwer, N.; Lobitz, S.; Daskalow, K.; Jons, T.; Vieth, M.; Schlag, P. M.; Kemmner, W.; Wiedenmann, B.; Cramer, T.; Hocker, M. HIF-1α determines the metastatic potential of gastric cancer cells. *Br. J. Cancer* **2009**, *100*, 772−781.
(20) Zhang, J.; Lu, A.; Li, L.; Yue, J.; Lu, Y. p16 Modulates VEGF expression via its interaction with HIF-1α in breast cancer cells. *Cancer Invest.* **2010**, *28*, 588−597.
(21) Akakura, N.; Kobayashi, M.; Horiuchi, I.; Suzuki, A.; Wang, J.; Chen, J.; Niizeki, H.; Kawamura, K.; Hosokawa, M.; Asaka, M. Constitutive expression of hypoxia-inducible factor-1α renders pancreatic cancer cells resistant to apoptosis induced by hypoxia and nutrient deprivation. *Cancer Res.* **2001**, *61*, 6548−6554.
(22) Cao, X.; Bloomston, M.; Zhang, T.; Frankel, W. L.; Jia, G.; Wang, B.; Hall, N. C.; Koch, R. M.; Cheng, H.; Knopp, M. V.; Sun, D. Synergistic antipancreatic tumor effect by simultaneously targeting hypoxic cancer cells with HSP90 inhibitor and glycolysis inhibitor. Clin. *Cancer Res.* **2008**, *14*, 1831−1839.
(23) Dang, D. T.; Chen, F.; Gardner, L. B.; Cummins, J. M.; Rago, C.; Bunz, F.; Kantsevoy, S. V.; Dang, L. H. Hypoxia-inducible factor-1α promotes nonhypoxia-mediated proliferation in colon cancer cells and xenografts. *Cancer Res.* **2006**, *66*, 1684−1693.
(24) Zhong, H.; De Marzo, A. M.; Laughner, E.; Lim, M.; Hilton, D. A.; Zagzag, D.; Buechler, P.; Isaacs, W. B.; Semenza, G. L.; Simons, J. W. Overexpression of hypoxia-inducible factor 1α in common human cancers and their metastases. *Cancer Res.* **1999**, *59*, 5830−5835.
(25) Li, L.; Lin, X.; Staver, M.; Shoemaker, A.; Semizarov, D.; Fesik, S. W.; Shen, Y. Evaluating hypoxia-inducible factor-1α as a cancer therapeutic target via inducible RNA interference in vivo. *Cancer Res.* **2005**, *65*, 7249−7258.
(26) Post, D. E.; Van Meir, E. G. A novel hypoxia inducible factor activated oncolytic adenovirus for cancer therapy. *Oncogene* **2003**, *22*, 2065−2072.
(27) Post, D. E.; Devi, N. S.; Li, Z.; Brat, D. J.; Kaur, B.; Nicholson, A.; Olson, J. J.; Zhang, Z.; Van Meir, E. G. Cancer therapy with a replicating oncolytic adenovirus targeting the hypoxic microenvironment of tumors. *Clin. Cancer Res.* **2004**, *10*, 8603−8612.
(28) Post, D. E.; Sandberg, E. M.; Devi, S. N.; Brat, D. J.; Xu, Z.; Tighiouart, M.; Van Meir, E. G. Targeted cancer-gene therapy using a HIF-dependent oncolytic adenovirus armed with interleukin-4. *Cancer Res.* **2007**, *67*, 6872−6881.
(29) Yang, L.; Cao, Z.; Li, F.; Post, D. E.; Van Meir, E. G.; Zhong, H.; Wood, W. C. Tumor-specific gene expression using the survivin promoter is further increased by hypoxia. *Gene Ther.* **2004**, *11*, 1215−23.
(30) Kim, H.-S.; Peng, G.-Y.; Hicks, J. M.; Weiss, H. L.; Van Meir, E. G.; Brenner, M. K.; Yotnda, P. Engineering human tumor-specific cytotoxic T cells to function in a hypoxic environment. *Mol. Ther.* **2008**, *16*, 599−606.
(31) Keith, B.; Johnson, R. S.; Simon, M. C. HIF1α and HIF2α: Sibling rivalry in hypoxic tumour growth and progression. *Nat. Rev. Cancer* **2012**, *12*, 9−22.
(32) Li, Z; Bao, S; Wu, Q; Wang, H; Eyler, C; Sathornsumetee, S; Shi, Q; Cao, Y; Lathia, J; McLendon, R. E.; Hjelmeland, A. B.; Rich, J. N. Hypoxia-inducible factors regulate tumorigenic capacity of glioma stem cells. *Cancer Cell* **2009**, *15*, 501−513.
(33) Qiang, L; Wu, T; Zhang, H. W.; Lu, N; Hu, R; Wang, Y. J.; Zhao, L; Chen, F. H.; Wang, X. T.; You, Q. D.; Guo, Q. L. HIF-1alpha is critical for hypoxia-mediated maintenance of glioblastoma stem cells by activating notch signaling pathway. *Cell Death Differ.* **2012**, *19*, 284−294.
(34) Kang, S. H.; Cho, H.; Devi, S. N.; Zhang, Z.; Escuin, D.; Liang, Z.; Mao, H.; Brat, D. J.; Olson, J. J.; Simons, J. W.; LaVallee, T. M.; Giannakakou, P.; Van Meir, E. G.; Shim, H. Anti-tumor effect of 2-methoxyestradiol in a rat orthotopic brain tumor model. *Cancer Res.* **2006**, *66*, 11992−11997.
(35) Koh, M. Y.; Spivak-Kroizman, T.; Venturini, S.; Welsh, S.; Williams, R. R.; Kirkpatrick, D. L.; Powis, G. Molecular mechanisms for the activity of PX-478, an antitumor inhibitor of the hypoxia-inducible factor-1α. *Mol. Cancer Ther.* **2008**, *7*, 90−100.
(36) Wang, X. H.; Cavell, B. E.; Syed Alwi, S. S.; Packham, G. Inhibition of hypoxia inducible factor by phenethyl isothiocyanate. *Biochem. Pharmacol.* **2009**, *78*, 262−272.
(37) Chau, N. M.; Rogers, P.; Aherne, W.; Carroll, V.; Collins, I.; McDonald, E.; Workman, P.; Ashcroft, M. Identification of novel small molecule inhibitors of hypoxia-inducible factor-1 that differentially block hypoxia-inducible factor-1 activity and hypoxia-inducible factor-1α induction in response to hypoxic stress and growth factors. *Cancer Res.* **2005**, *65*, 4918−4928.
(38) Lee, K; Lee, J. H.; Boovanahalli, S. K.; Jin, Y.; Lee, M.; Jin, X.; Kim, J. H.; Hong, Y. S.; Lee, J. J. Aryloxyacetylamino)benzoic acid analogs: A new class of hypoxia-inducible factor-1 inhibitors. *J. Med. Chem.* **2007**, *50*, 1675−1684.
(39) Semenza, G. L. Evaluation of HIF-1 inhibitors as anticancer agents. *Drug Discovery Today* **2007**, *12*, 853−859.
(40) Tan, C.; de Noronha, R. G.; Roecker, A. J.; Pyrzynska, B.; Khwaja, F.; Zhang, Z.; Zhang, H.; Teng, Q.; Nicholson, A. C.; Giannakakou, P.; Zhou, W.; Olson, J. J.; Pereira, M. M.; Nicolaou, K. C.; Van Meir, E. G. Identification of a novel small-molecule inhibitor of the hypoxia-inducible factor 1 pathway. *Cancer Res.* **2005**, *65*, 605−612.
(41) Belozerov, V.; Van Meir, E. G. Hypoxia Inducible factor-1: A novel target for cancer therapy. *Anti-Cancer Drugs* **2005**, *16*, 901−909.
(42) Belozerov, V.; Van Meir, E. G. Inhibitors of hypoxia inducible factor-1 signaling. *Curr. Opin. Invest. Drugs* **2006**, *7*, 1067−1076.
(43) Cook, K. M.; Hilton, S. T.; Mecinovic, J.; Motherwell, W. B.; Figg, W. D.; Schofield, C. J. Epidithiodiketopiperazines block the interaction between hypoxia-inducible factor-1alpha (HIF-1alpha) and p300 by a zinc ejection mechanism. *J. Biol. Chem.* **2009**, *284*, 26831−26838.
(44) Kung, A. L.; Zabludoff, S. D.; France, D. S.; Freedman, S. J.; Tanner, E. A.; Vieira, A.; Cornell-Kennon, S.; Lee, J.; Wang, B.; Wang, J.; Memmert, K.; Naegeli, H. U.; Petersen, F.; Eck, M. J.; Bair, K. W.; Wood, A. W.; Livingston, D. M. Small molecule blockade of transcriptional coactivation of the hypoxia-inducible factor pathway. *Cancer Cell* **2004**, *6*, 33−43.
(45) Lee, K; Zhang, H; Qian, D. Z.; Rey, S; Liu, J. O.; Semenza, G. L. Acriflavine inhibits HIF-1 dimerization, tumor growth, and vascularization. *Proc. Natl. Acad. Sci. U. S. A.* **2009**, *106*, 17910−17915.
(46) Tan, C.; de Noronha, R. G.; Devi, N. S.; Jabbar, A. A.; Kaluz, S.; Liu, Y.; Reid-Mooring, S.; Nicolaou, K. C.; Wang, B.; Van Meir, E. G. Sulfonamides as a new scaffold for hypoxia inducible factor pathway inhibitors. *Bioorg. Med. Chem. Lett.* **2011**, *21*, 5528−5532.
(47) Nicolaou, K. C.; Pfefferkorn, J. A.; Roecker, A. J.; Cao, G.-Q.; Barluenga, S.; Mitchell, H. J. Natural product-like combinatorial libraries based on privileged structures. 1. General principles and solid-phase synthesis of benzopyrans. *J. Am. Chem. Soc.* **2000**, *122*, 9939−9953.
(48) Nicolaou, K. C.; Pfefferkorn, J. A.; Mitchell, H. J.; Roecker, A. J.; Barluenga, S.; Cao, G.-Q.; Affleck, R. L.; Lillig, J. E. Natural product-like combinatorial libraries based on privileged structures. 2. Construction of a 10 000-membered benzopyran library by directed split-and-pool chemistry using nanokans and optical encoding. *J. Am. Chem. Soc.* **2000**, *122*, 9954−9967.
(49) Narita, T.; Yin, S.; Gelin, C. F.; Moreno, C. S.; Yepes, M.; Nicolaou, K. C.; Van Meir, E. G. Identification of a novel small molecule HIF-1a translation inhibitor. *Clin. Cancer Res.* **2009**, *15*, 6128−36.
(50) Shi, Q.; Yin, S.; Kaluz, S.; Ni, N.; Devi, N. S.; Mun, J.; Wang, D.; Damera, K.; Chen, W.; Burroughs, S.; Reid-Mooring, S.; Goodman, M.

M.; Van Meir, E. G.; Wang, B.; Snyder, J. P. Binding model for the interaction of anti-cancer arylsulfonamides with the p300 Transcription co-factor. *ACS Med. Chem. Lett.* **2012**, in press.
(51) Yin, S.; Kaluz, S.; Devi, N. S.; Jabbar, A. A.; de Noronha, R. G.; Mun, J.; Zhang, Z.; Boreddy, P. R.; Wang, W.; Wang, Z.; Abbruscato, T.; Chen, Z.; Olson, J. J.; Zhang, R.; Goodman, M. M.; Nicolaou, K. C.; Van Meir, E. G. Arylsulfonamide KCN1 inhibits in vivo glioma growth and interferes with HIF signaling by disrupting HIF-1α interaction with co-factors p300/CBP. Unpublished results.
(52) Wang, W.; Rayburn, A. L.; Xu, E. R.; Zhang, H.; Zhang, X.; Wang X.; Wang, M. H.; Wang, H.; Van Meir, E, G.; Zhang, R. KCN1, a novel synthetic sulfonamide anticancer agent: In vitro and in vivo anti-pancreatic cancer activities and preclinical pharmacology. Unpublished results.
(53) Zhang, Q.; Kaluz, S.; Yang, H.; Van Meir, E. G.; Grossniklaus, H. E. Efficacy of the novel small molecule HIF pathway inhibitor KCN1 in the control of micrometastases in experimental ocular melanoma. Unpublished results.
(54) Mun, J.; Jabbar, A.; Devi, N.; Liu, Y.; Van Meir, E. G.; Goodman, M. M. Structure−activity relationship of 2,2-dimethyl-2*H*-chromene based arylsulfonamide analogs of 3,4-dimethoxy-*N*-[(2,2-dimethyl-2*H*-chromen-6-yl)methyl]-*N*-phenylbenzenesulfonamide, a novel small molecule hypoxia inducible factor-1 (HIF-1) pathway inhibitor and anti-cancer agent. *Bioorg. Med. Chem.* [Online early access]. DOI:10.1016/j.bmc.2012.04.064.
(55) Oprea, T. I. Current trends in lead discovery: Are we looking for the appropriate properties? *Mol. Diversity* **2000**, *5*, 199−208.
(56) Perola, E. An analysis of the binding efficiencies of drugs and their leads in successful drug discovery programs. *J. Med. Chem.* **2010**, *53*, 2986−2997.
(57) VCCLAB, Virtual computational chemistry laboratory, http://www.vcclab.org, 2005.
(58) Tetko, I. V.; Gasteiger, J.; Todeschini, R.; Mauri, A.; Livingstone, D.; Ertl, P.; Palyulin, V. A.; Radchenko, E. V.; Zefirov, N. S.; Makarenko, A. S.; Tanchuk, V. Y.; Prokopenko, V. V. Virtual computational chemistry laboratory—Design and description. *J. Comput. Aid. Mol. Des.* **2005**, *19*, 453−463.
(59) Tetko, I. V. Computing chemistry on the web. *Drug Discovery Today* **2005**, *10*, 1497−1500.
(60) Tetko, I. V.; Tanchuk, V. Y. Application of associate neutral networks for prediction of lipophilicity in ALOGPS 2.1 program. *J. Chem. Inf. Comput. Sci.* **2002**, *42*, 1136−1145.
(61) Tetko, I. V.; Tanchuk, V. Y.; Villa, A. E. Prediction of *n*-octanol/water partition coefficients from PHYSPROP database using artificial neural networks and E-state indices. *J. Chem. Inf. Comput. Sci.* **2001**, *41*, 1407−1421.
(62) Tetko, I. V.; Tanchuk, V. Y.; Kasheva, T. N.; Villa, A. E. Estimation of aqueous solubility of chemical compounds using E-state indices. *J. Chem. Inf. Comput. Sci.* **2001**, *41*, 1488−1493.
(63) Smith, L. R.; Mahoney, N.; Molyneux, R. J. Synthesis and structure−phytotoxicity relationships of acetylenic phenols and benzopyrane metabolites, and their analogues, from the grapevine pathogen *Eutypa lata*. *J. Nat. Prod.* **2003**, *66*, 169−176.
(64) Roblin, R. O., Jr.; Clapp, J. W. The preparation of heterocyclic sulfonamides. *J. Am. Chem. Soc.* **1950**, *72*, 4890−4892.
(65) Karino, H.; Goda, H.; Sakamoto, J.; Yoshida, K.; Nishiguchi, H. Process for preparing aromatic or heteroaromatic sulfonyl halides. U.S. patent 5,811,571. Sep 22, 1998.
(66) Wright, S. W.; Hallstrom, K. N. A Convenient preparation of heteroaryl sulfonamides and sulfonyl fluorides from heteroaryl thiols. *J. Org. Chem.* **2006**, *71*, 1080−1084.
(67) Hanessian, S.; Kagotani, M.; Komaglou, K. Design and reactivity of organic functional groups—2-Pyridylsulfonates as nucleofugal esters: Remarkably mild transformations into halides and olefins. *Heterocycles* **1989**, *28*, 1115−1120.
(68) Diltz, S.; Aguirre, G.; Ortega, F.; Walsh, P. J. Synthesis of chiral heteroaromatic tetradentate sulfonamide based ligands. *Tetrahedron: Asymmetry* **1997**, *8*, 3559−3562.
(69) Crombie, L.; Bandaranayake, W. M.; Whiting, D. A. 2-Hydroxy-3-methyl-1,1-dimethoxybutane, new reagent for dimethylbenzopyranylation. Synthesis of lonchocarpin, jacareubin, evodionol methyl ether, and other benzopyranes. *J. Chem. Soc. (C)* **1971**, *4*, 811−816.
(70) Crombie, L.; Bandaranayake, W. M.; Whiting, D. A. Novel methods for the synthesis of 2,2-dimethylbenzopyranes. *J. Chem. Soc. (D), Chem. Commun.* **1969**, *17*, 970−971.
(71) Henry, G. E.; Jacobs, H. A short synthesis of 5-methoxy-2,2-dimethyl-2*H*-1-benzopyran-6-propanoic acid methyl ester. *Tetrahedron* **2001**, *57*, 5335−5338.
(72) OECD guidelines for the testing of chemicals. Partition coefficient (*n*-octanol/water): Shake flask method. 107, Adopted July 27, 1995. OECD guidelines for the testing of chemicals. Partition coefficient (*n*-octanol/water), high performance liquid chromatography (HPLC) method. 117, Adopted April 13, 2004.
(73) Rodriguez-Lopez, V.; Moreno-Escobar, J. A.; Avila-Torres, O.; Tlahuext, H. 6-Acetyl-5-hydroxy-2,2-dimethyl-2*H*-chromene. *Acta Crystallogr.* **2006**, *E62*, o3616−o3617.
(74) Orgala, J.; Erdelmeier, C. A. J.; Wright, A. D.; Rali, T.; Sticher, O. Two chromenes and a prenylated benzoic acid derivative from *Piper aduncum*. *Phytochemistry* **1993**, *34*, 813−818.
(75) Batista, J. M., Jr.; Lopes, A. A.; Ambrosio, D. L.; Regasini, L. O.; Kato, M. J.; Bolzani, V. S.; Cicarelli, R. M. B.; Furlan, M. Natural chromenes and chromene derivatives as potential anti-trypanosomal agents. *Biol. Pharm. Bull.* **2008**, *31*, 538−540.
(76) Johnson, A. J.; Kumar, R., A.; Rasheed, S. A.; Chandrika, S. P.; Chandrasekhar, A.; Baby, S.; Subramoniam, A. Antipyretic, analgesic, anti-inflammatory and antioxidant activities of two major chromenes from *Melicope lunu-ankenda*. *J. Ethnopharmacol.* **2010**, *130*, 267−271.
(77) Dragovich, P. S.; Prins, T. J.; Zhou, R.; Johnson, T. O.; Hua, Y.; Luu, H. T.; Sakata, S. K.; Brown, E. L.; Maldonado, F. C.; Tuntland, T.; Lee, C. A.; Fuhrman, S. A.; Zalman, L. S.; Patick, A. K.; Matthews, D. A.; Wu, E. Y.; Guo, M.; Borer, B. C.; Nayyar, N. K.; Moran, T.; Chen, L.; Rejto, P. A.; Rose, P. W.; Guzman, M. C.; Dovalsantos, E. Z.; Lee, S.; Gleeson, J.-P. R.; Wu, Z. P.; Liu, J.; Meador, J. W., III; Ferre, R. A. Structure-based design, synthesis, and biological evaluation of irreversible human rhinovirus 3C protease inhibitors. 8. Pharmacological optimization of orally bioavailable 2-pyridone-containing peptidomimetics. *J. Med. Chem.* **2003**, *46*, 4572−4585.
(78) Perez, R. P.; Godwin, A. K.; Handel, L. M.; Hamilton, T. C. A. Comparison of clonogenic, microtetrazolium and sulforhodamine B assays for determination of cisplatin cytotoxicity in human ovarian carcinoma cell lines. *Eur. J. Cancer* **1993**, *29A*, 395−399.
(79) Vichai, V.; Kirtikara, K. Sulforhodamine B colorimetric assay for cytotoxicity screening. *Nat. Protocols* **2006**, *3*, 1112−1116.